This is to certify that the

thesis entitled

THE SYNTHESIS AND CHARACTERIZATION

OF A NOVEL MOLYBDENUM-IRON-SULFUR CLUSTER

presented by

Paul Ernest Lamberty

has been accepted towards fulfillment
of the requirements for

Masters degree in Chemistry

Carl H. Brubaker, Jr.
Major professor

Date 5-11-83

THE SYNTHESIS AND CHARACTERIZATION OF A NOVEL MOLYBDENUM-IRON-SULFUR CLUSTER

By

Paul Ernest Lamberty

A THESIS

Submitted to
Michigan State University
in partial fulfillment of the requirement
for the degree of

MASTER OF SCIENCE

Department of Chemistry

1983

ABSTRACT

THE SYNTHESIS AND CHARACTERIZATION OF A NOVEL MOLYBDENUM-IRON-SULFUR CLUSTER

By

Paul Ernest Lamberty

Reaction of three equivalents of $Fe_2S_2(CO)_6^{2-}$ in tetrahydrofuran with one equivalent of molybdenum pentachloride in acetonitrile at -78°C affords a novel molybdenum-iron-sulfur cluster containing a 1:6 molybdenum to iron ratio. The complex has the formulation $[MoFe_6S_6(CO)_{18}]^{2-}$, and has been isolated as the 1,2-ethylenebis(triphenylphosphonium) and benzyltriethylammonium salts.

The optical spectrum shows absorptions at: λ_{max}: 327, 459, 572 (sh), 668 (sh). The infrared spectrum shows peaks at 2070, 2037, 1990 cm^{-1} in the carbonyl stretching region. Electrochemical measurements indicate one quasi-reversible oxidation and two reductions, one of which is reversible. Conductivity measurements support the formation of the complex as a dianion. Mossbauer spectra have been recorded at 4.2 K in a 600 G magnetic field, and indicate that all iron atoms are equivalent, giving only a simple quadrupole doublet.

Magnetic susceptibility measurements show that the compound exhibits an unusually large magnetic moment (μ_{eff} = 4.85 BM) and slight temperature-independent-paramagnetism.

Attempts to obtain crystals suitable for an X-ray structure determination have met with little success; possible solutions for the problems encountered are discussed.

To My Family:

Robert, Margaret, John and Thomas

And to Jan, a very special friend

Thank you.

ACKNOWLEDGMENTS

I would like to gratefully thank Professor Bruce A. Averill for his advice and guidance throughout my graduate career. His knowledge of synthetic inorganic chemistry and insight on the interpretation of the results have been invaluable.

I would like to acknowledge Dr. E. Münck and Dr. T. A. Kent for obtaining the Mössbauer data and Walter E. Cleland, Jr. for his aid with running the electrochemistry experiments.

I would like to thank Walter E. Cleland, Jr., Jim Davis, Mark Antonio, Vijay Kumar, and my other co-workers for their friendship and advice on matters pertaining to my research and graduate career.

Special thanks are extended to the Department of Chemistry for providing a teaching assistantship and the University of Virginia for support during my last term.

I would also like to thank Professors Brubaker, Eick, and Babcock for serving on my committee.

And last, special thanks to Mrs. P. Warstler for the typing of this thesis, to Mrs. J. Moore for her much appreciated secretarial help, and to Jo Kotarski for her excellent work on the graphics.

TABLE OF CONTENTS

Chapter			Page
LIST OF TABLES.			vi
LIST OF FIGURES			vii
LIST OF ABBREVIATIONS			x
I.	INTRODUCTION		1
II.	EXPERIMENTAL		12
	A.	Materials.	12
	B.	Methods.	15
	C.	Syntheses.	16
		1. Preparation of μ-Dithiobis-tricarbonyliron)	16
		2. Preparation of $(BzEt_3N)_2$-$[MoFe_6S_6(CO)_{18}]$.	17
		3. Preparation of $[Ph_3PCH_2CH_2PPh_3]$-$[MoFe_6S_6(CO)_{18}]$.	19
III.	RESULTS AND DISCUSSION		20
	A.	Synthesis.	20
	B.	Solution Conductivity.	25
	C.	Infrared Spectroscopy.	28
	D.	Electronic Spectroscopy.	33
	E.	Mössbauer Spectroscopy	38
	F.	Magnetic Susceptibility.	47
	G.	Electrochemistry	53

Chapter Page

H. X-ray Structural Studies 62

IV. CONCLUSIONS. 65

REFERENCES. 66

LIST OF TABLES

Table		Page
I	Elemental Analysis Data for the 1,2-Ethylenebis(triphenylphosphonium) and Benzyltriethylammonium salts of $[MoFe_6S_6(CO)_{18}]^{2-}$.	21
II	Solution Conductivity Data Obtained in Acetonitrile.	27
III	Infrared Spectroscopic Data in Carbonyl Stretching Region.	32
IV	Electronic Spectroscopic Data for $[MoFe_6S_6(CO)_{18}]^{2-}$ and $Fe_2S_2(CO)_6$	36
V	Absorption Spectra of Some Non-oxo, 6-Coordinate Molybdenum (IV) Complexes.	37
VI	Mössbauer Data for $[MoFe_6S_6(CO)_{18}]^{2-}$, $Fe_2S_2(CO)_6$, and Other Iron Compounds . . .	46
VII	Electrochemical Data for $[MoFe_6S_6(CO)_{18}]^{2-}$.	55
VIII	Electrochemical Data for Other Compounds.	61

LIST OF FIGURES

Figure		Page
I	Schematic representation of the proposed models for the iron-molybdenum cofactor.	5
II	Schematic representation of the structurally characterized $MoFe_3S_4$ cubane clusters prepared to date	8
III	Schematic representation of the linear molybdenum-iron-sulfur clusters prepared to date.	10
IV	Reaction scheme for the formation of $[MoFe_6S_6(CO)_{18}]^{2-}$. Generation of $Fe_2S_2(CO)_6^{2-}$ was accomplished with $LiEt_3BH$, after which one equivalent of molybdenum pentachloride was added to every three equivalents of $Fe_2S_2(CO)_6^{2-}$.	23
V	Infrared spectra of $[MoFe_6S_6(CO)_{18}]^{2-}$, (top), and $Fe_2S_2(CO)_6$ in acetonitrile at 20°C. Calibrated with polystyrene film	30
VI	Optical spectra of $[MoFe_6S_6(CO)_{18}]^{2-}$, (solid line), and $Fe_2S_2(CO)_6$ in aceto-nitrile solution at 20°C	35

Figure		Page
VII	Approximate ranges of isomer shifts observed in iron compounds relative to metallic iron at room-temperature. S refers to the spin quantum number. . . .	41
VIII	Mössbauer spectrum of $[MoFe_6S_6(CO)_{18}]^{2-}$ as a polycrystalline sample diluted with boron nitride. Recorded at 4.2 K with a 600 G magnetic field.	43
IX	Mössbauer spectrum of $Fe_2S_2(CO)_6$ as a polycrystalline sample diluted with boron nitride. Recorded at 4.2 K with a 600 G magnetic field.	45
X	Magnetic susceptibility of $(BzEt_3N)_2$-$[MoFe_6S_6(CO)_{18}]$ as a function of temperature in the solid state, obtained in a 2.000 kG magnetic field. Units for χ_m are $EMU \cdot M^{-1}$	51
XI	Inverse of magnetic susceptibility of $(BzEt_3N)_2[MoFe_6S_6(CO)_{18}]$, $(M \cdot EMU^{-1})$, as a function of temperature. Slight downward slope is due to temperature-independent-paramagnetism. Obtained in a 2.000 kG magnetic field	53

Figure Page

XII Differential pulse polarogram of first and second electrochemical reductions of $[MoFe_6S_6(CO)_{18}]^{2-}$. 57

XIII Cyclic voltammograms of the first reduction process (top), and the oxidation process of $[MoFe_6S_6(CO)_{18}]^{2-}$. Scan rate: 100 mV/sec 59

XIV Schematic representation of the proposed structure for $[MoFe_6S_6(CO)_{18}]^{2-}$. Compound has been isolated as $(BzEt_3N)^+$ and $(Ph_3PCH_2CH_2PPh_3)^{2+}$ salts 63

LIST OF ABBREVIATIONS

Solvents:

MeCN	= acetonitrile
EtCN	= propionitrile
MeOH	= methanol
EtOH	= ethanol
Et_2O	= diethyl ether
i-ProH	= isopropanol
THF	= tetrahydrofuran
DME	= dimethoxethane

Reagents:

KOH	= potassium hydroxide
$MoCl_5$	= molybdenum pentachloride
$MoCl_4$	= α-molybdenum tetrachloride
$Fe(CO)_5$	= iron pentacarbonyl
Na_2S	= sodium sulfide
Na_2S_5	= sodium polysulfide
$Fe_2S_2(CO)_6$	= μ-dithiobis(tricarbonyliron)
$LiEt_3BH$	= lithium triethylborohydride

Miscellaneous:

$Fe_2S_2(CO)_6^{2-}$	= μ-dithiobis(tricarbonyliron) dianion
$[Ph_3PCH_2CH_2PPh_3]^{2+}$	= 1,2-ethylenebis(triphenylphosphonium)
$BzEt_3N$	= benzyltriethylammonium
BM	= Bohr magneton
SCE	= standard calomel electrode
Ph	= phenyl
Ph_4As^+	= tetraphenylarsonium

I. INTRODUCTION

The limiting factor in agricultural production is the supply of fixed nitrogen. Every year over 40 million tons of anhydrous ammonia fertilizer are produced to supply the demands of our nation's farmers. Ammonia is manufactured industrially via the Haber-Bosch process,[1] which utilizes high temperatures (ca. 450°C) and high pressures (ca. 350 atm). In order to manufacture ammonia on an industrial scale, very large amounts of energy are consumed, most of which is obtained from the use of fossil fuels.

Because of the decreased supply and increased cost of fossil fuels, research has been focussed on developing potential alternative processes for ammonia production. Recently, much attention has been given to the metalloenzyme, nitrogenase, which is responsible for biological nitrogen fixation and has the unique and valuable property of catalyzing the reduction of nitrogen gas to ammonia at ambient temperature and pressure. The exact mechanism of this reduction is not known, but knowledge is slowly being accumulated through many approaches, one of which is the construction of synthetic models for the metal centers of nitrogenase.

The enzyme is known to consist of two oxygen-sensitive

components, an iron protein and a molybdenum-iron protein. The iron protein (m.w. 60,000) contains four iron and four sulfide atoms per molecule. Spectroscopic and cluster extrusion experiments indicate that the iron and sulfur are present in a Fe_4S_4 cluster arrangement.[2,3]

The molybdenum-iron protein (m.w. ~220,000) contains approximately 32 iron atoms, 30±2 sulfides, and 2 molybdenum atoms per molecule.[2] It has been found that four of the metal components of the molybdenum-iron protein consist of Fe_4S_4 units. The rest of the iron and sulfur and all of the molybdenum is contained within a low-molecular weight cofactor.[4] This cofactor, which can be removed from the molybdenum-iron protein, contains six to eight iron atoms and approximately ten sulfides per molybdenum atom and constitutes a novel cluster. The low-temperature (6-20 K) EPR spectrum of the cofactor shows an axial signal[5] with slight rhombic distortion (g-values 2.0, 3.65, and 4.3). This has been shown to originate from one of the Kramer's doublets of an S = 3/2 system.[5,6] Low temperature ^{57}Fe Mössbauer spectra of the isolated cofactor[7] are similar to the spectra assigned to the cofactor centers of the molybdenum-iron protein, except for slight broadening of the lines and for the presence of a small quadrupole doublet ($\Delta E_Q \simeq 0.9$ mm/sec., $\delta \simeq 0.4$ mm/sec.), which suggests that approximately twenty percent of the total iron is present in another environment. Analysis of

the spectrum of the metal centers in the native protein has shown the presence of six iron atoms in each S = 3/2 metal center,[8] in agreement with the presence of six irons per molybdenum in the cofactor. Mo K-edge extended X-ray absorption fine structure (EXAFS) spectroscopy indicates two or three iron atoms at approximately 2.71 Å and four or five sulfur atoms at approximately 2.35 Å as nearest neighbors to the molybdenum. Recently Fe-edge EXAFS studies[9] indicate that the iron atoms in the cofactor have an average of 3.4 ± 1.6 sulfur atoms at 2.25 Å, 2.3 ± 0.9 iron atoms at 2.66 Å, 0.4 ± 0.1 molybdenum atoms at 2.76 Å, and 1.2 ± 1.0 oxygen atoms at 1.81 Å as nearest neighbors.

Thus far, available evidence concerning the actual mechanism of reduction of dinitrogen to ammonia indicates that electrons are transferred from an external reductant (reduced ferredoxin or dithionite) to the iron protein to the molybdenum-iron protein to substrate.[2] Therefore, it is believed that the substrate coordinates to and is reduced at the iron-molybdenum cofactor within the molybdenum-iron protein.

Due to the extreme oxygen sensitivity of and problems in purifying the cofactor, its structure has not yet been determined. However, a number of structural models have been proposed; see Figure I. Until recently, no synthetic molybdenum-iron-sulfur clusters were known, making it difficult to assess the validity of the proposed structures.

Figure I. Schematic representation of the proposed models for the iron-molybdenum cofactor.

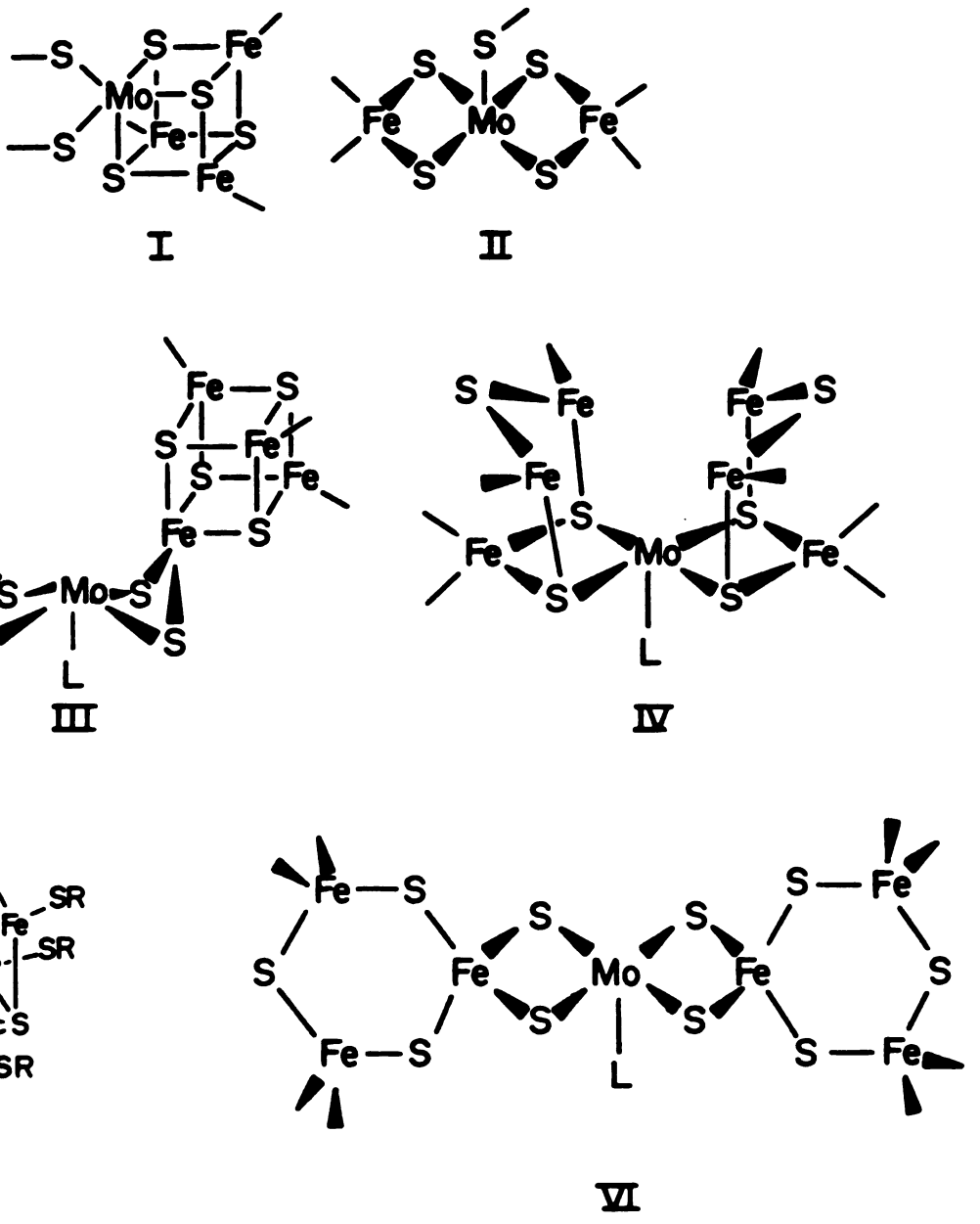

Figure I

By synthesizing and characterizing molybdenum-iron-sulfur clusters the inorganic chemist hopes to provide a body of data, which upon comparison with corresponding data obtained for the cofactor, will contribute to an eventual elucidation of the structure of the iron-molybdenum cofactor and the mechanism of action of nitrogenase. Synthetic efforts have thus far led to two classes of molybdenum-iron-sulfur clusters: the "cubane" complexes and the "linear" type clusters.

Examples of "cubane" clusters include:[10-27] $[Fe_6Mo_2S_3(SR)_9]^{3-}$, $[Fe_6Mo_2S_9(SR)_8]^{3-}$, $[Fe_7Mo_2S_8(SR)_{12}]^{3-,4-}$, and $[Fe_4MoS_4(SR)_3(C_6H_4O_2)_3]^{3-}$, presented in Figure II, all of which contain the Fe_3MoS_4 core unit. EXAFS studies on these compounds show that the Mo-Fe and Mo-S (bridging) distances are virtually identical to that of the Mo site of nitrogenase,[10,28,29] and the observed ^{57}Fe Mossbauer isomer shifts and quadrupole splittings are close to those reported for the iron-molybdenum cofactor.[7,30] But these are not detailed models for the cofactor due to improper stoichiometry (3 Fe/Mo and too much $S^{=}$) and none of these compounds exhibit EPR spectra that approximate that of the cofactor.

The "linear" class include: $[FeMoS_4X_2]^{2-}$ (X = SAr, OAr, Cl), $[Fe_2MoS_6X_2]^{3-}$ (X = SAr, $X_2 = S_5$), $[Fe(MoS_4)_2]^{3-}$ and $[Fe_2MoS_4Cl_2]^{2-}$,[31-37] shown in Figure III. These also do not constitute accurate models for the iron-molybdenum

Figure II. Schematic representation of the structurally characterized $MoFe_3S_4$ cubane clusters prepared to date.

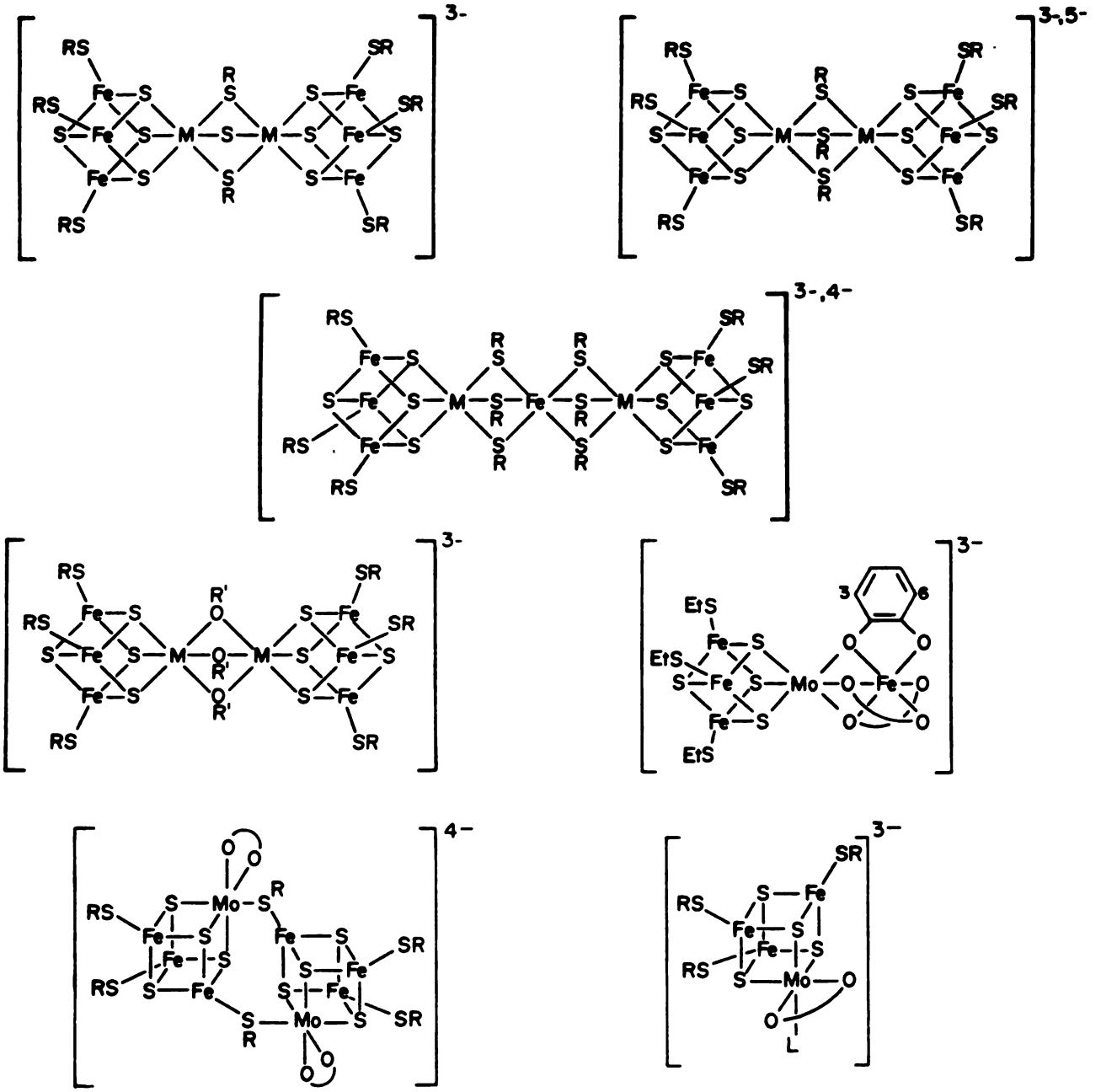

Figure II

Figure III. Schematic representation of the linear molybdenum-iron-sulfur clusters prepared to date.

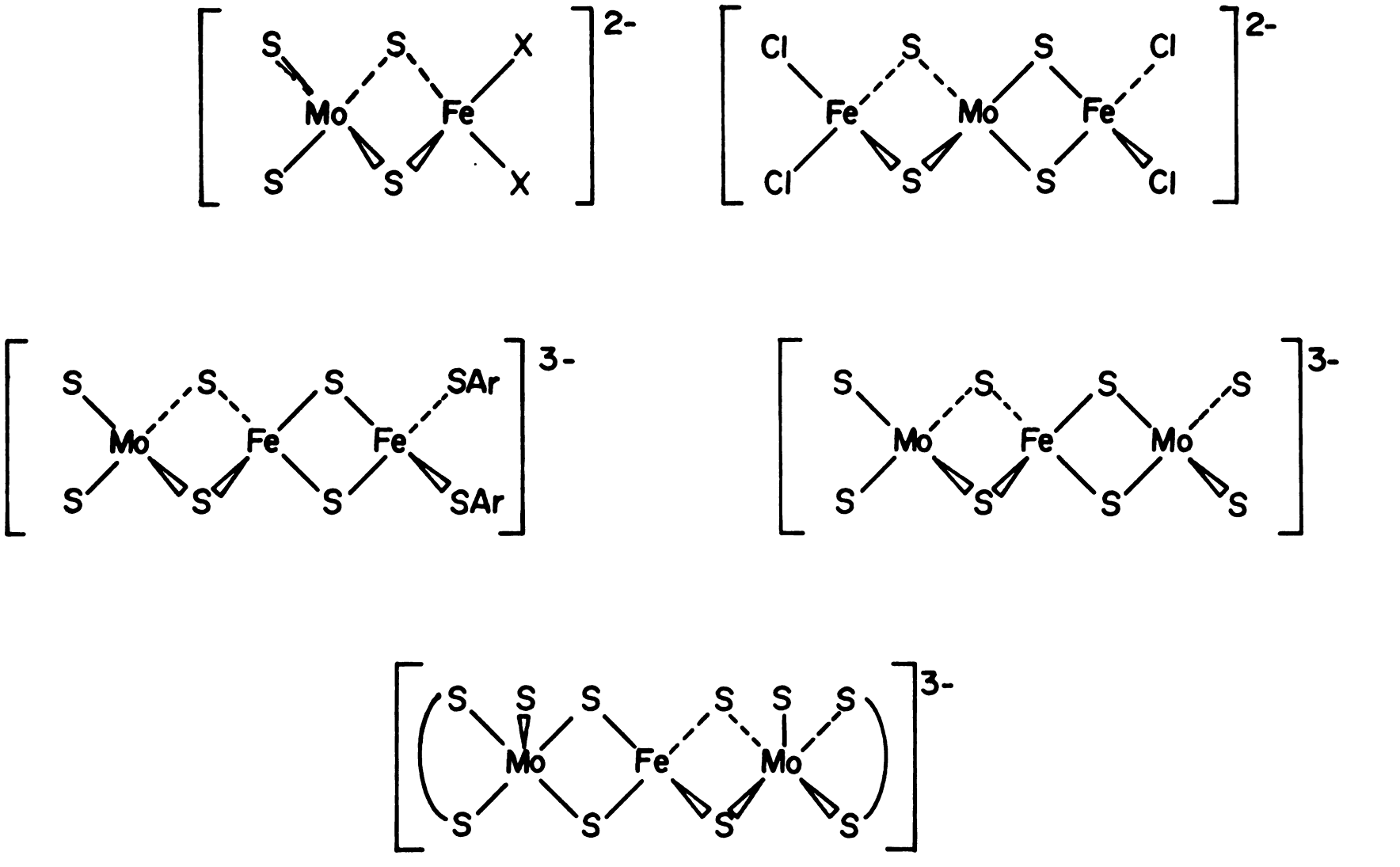
S
S
X
Mo
Fe
S
S
X
2-
Cl
S
S
Cl
Fe
Mo
Fe
Cl
S
S
Cl
2-
S
S
S
SAr
Mo
Fe
Fe
S
S
S
SAr
3-
S
S
S
S
Mo
Fe
Mo
S
S
S
S
3-
S
S
S
S
S
S
Mo
Fe
Mo
S
S
S
S
3-

Figure III

cofactor, since the oxidation state of Mo (+6) is too high and EXAFS studies indicate the Mo-S distance is too short.

Both the "linear" and "cubane" cluster syntheses utilize tetrathiomolybdate (MoS_4^{2-}) as a starting material, which significantly limits the resulting chemistry. Therefore, new types of starting materials must be found in order to provide synthetic routes to molybdenum-iron-sulfur clusters with structures other than the linear MoS_2Fe or cubane $MoFe_3S_4$ units (possibly including a synthetic analog of the iron-molybdenum cofactor).

The research described in this thesis deals with the synthesis and characterization of a new molybdenum-iron-sulfur cluster containing the approximate ratio of Fe:Mo:S that is present in the iron-molybdenum cofactor. This cluster, although not a detailed model for the cofactor, does represent a new structural class of molybdenum-iron-sulfur cluster, and has possibilities for utilization as a starting material for the preparation of more realistic models for the iron-molybdenum cofactor.

II. EXPERIMENTAL

A. Materials

All operations were performed in an atmosphere of nitrogen gas, purified by passage over hot BASF R-3-11 catalyst to remove oxygen and through Aquasorb (supported phosphorus pentoxide) to remove moisture. Solvents and solutions were degassed prior to use by repeated evacuation and flushing with purified nitrogen gas. Acetonitrile and propionitrile were distilled from calcium hydride and redistilled from phosphorus pentoxide. Tetrahydrofuran and ethyl ether were distilled from lithium aluminum hydride. Isopropanol and methanol were distilled from aluminum isopropoxide and magnesium methoxide, respectively. Carbon tetrachloride was distilled from phosphorus pentoxide, and tetrachloroethylene was dried over 4 Å molecular sieves.

1,2-Ethylenebis(triphenylphosphonium) bromide was purchased from Strem Chemicals, Inc. and was recrystallized from ethyl acetate. Lithium triethylborohydride, "Super Hydride", was purchased from Aldrich Chemical Co. as a 1.0 M solution in THF. This was assayed by measuring the amount of hydrogen formed upon reaction with a water-glycerin mixture. Molybdenum pentachloride was purchased

from Alfa Products Inc. as a 99+%, resublimed, no further purification was necessary. All other reagents were of commercial reagent grade and used without further purification.

Benzyltriethylammonium chloride was obtained from Walter E. Cleland, Jr.

$[Cr(en)_3][Ph_4B]_3$ was obtained from Robert H. Tieckelmann.

Tetrabutylammonium perchlorate was prepared from tetrabutylhydroxide and perchloric acid, and recrystallized from water and methanol.

$(Et_4N)_2MoS_4$ was prepared by a metathesis reaction from $(NH_4)_2MoS_4$ and $2(Et_4N)Cl$.[12] A 1000 ml., round-bottomed, side arm flask equipped with a stir bar was charged with 30 g $(NH_4)_2MoS_4$ and 40.1 g $(Et_4N)Cl$ and ~700 ml degassed acetonitrile was added. The resulting suspension was allowed to stir for 18 hours, after which it was filtered in air using a medium glass frit. The filtrate was collected along with several washings and evaporated to dryness using a rotary evaporator and a room temperature water bath. The product was collected as reddish-orange crystals. Optical spectrum showed peaks at 473 nm, 322 nm, and 244 nm. If a peak at 400 nm due to the oxo species, $MoOS_3^=$, was observed, the product was purified by recrystallization from acetonitrile/ether.

Molybdenum tetrachloride was prepared by the published[38]

procedure.

$$2MoCl_5 + Cl_2C{=}CCl_2 \xrightarrow{CCl_4} 2MoCl_4 + Cl_3C{-}CCl_3$$

A 250 ml, round-bottomed, side arm flask was charged with 8.0 g $MoCl_5$. 100 ml degassed carbon tetrachloride and 40 ml degassed tetrachloroethylene were added via cannula. The flask was then equipped with a reflux condenser and an external mercury bubbler (with trap). The mixture was heated to reflux for 2.5 days. After cooling the mixture was filtered, washed with carbon tetrachloride, and vacuum dried. The product was collected as dark black microcrystals. The X-ray powder pattern showed intense d spacings of 6.18, 5.97, 4.50, 4.07, 3.30, 2.88, 2.60, 2.56, 2.22, 2.11, 2.02. Literature[38] (d,I) values: 9.092, 5; 6.099, 100; 5.888, 100; 5.383, 5; 5.274, 5; 5.091, 10; 4.866, 10; 4.618, 10; 4.444, 80; 4.386, 5; 4.042, 80; 3.266, 30; 2.936, 5; 2.856, 30; 2.750, 5; 2.705, 5; 2.632, 100; 2.602, 25; 2.522, 25; 2.491, 2; 2.365, 2; 2.320, 2; 2.270, 2; 2.221, 50; 2.184, 20; 2.131, 20; 2.102, 50; 2.075, 1; 2.012, 50; 1.961, 2; 1.897, 5; 1.863, 5; 1.838, 30; 1.811, 2; 1.753, 20 1.721, 40; 1.679, 1; 1.633, 30; 1.586, 30; 1.572, 2; 1.506, 10; 1.467, 10; 1.457, 2; 1.385, 5; 1.374, 5; 1.348, 2; 1.336, 2.

B. Methods

Optical spectra were recorded by means of a Cary Model 17 or Cary Model 219 spectrophotometer. Infrared spectra were obtained with a Perkin-Elmer Model 457 or Model 237B grating infrared spectrophotometer by using sodium chloride or potassium bromide solution cells. Variable temperature magnetic susceptibility measurements were performed on a SHE Corporation SQUID susceptometer opterating at 2 KG. Room temperature magnetic susceptibility measurements were also performed with an Alpha Faraday balance using Hg-$[Co(SCN)_4]$ as a calibrant. Electrochemical measurements were made with a PAR Model 174A polarographic analyzer employing either dc polarography (dropping mercury electrode) or cyclic voltammetry (glassy carbon electrode). Mössbauer spectra were measured by Dr. T. Kent and Prof. E. Münck at the Grey Freshwater Biology Institute, University of Minnesota, Navarre, Minnesota. Isomer shifts are reported vs. metallic iron foil at room temperature.[39] Conductivity measurements were obtained using a Markson "ElectroMark" Analyzer. Melting points were obtained by using sealed capillaries in vacuo and are uncorrected. Elemental analyses were performed by Galbraith Laboratories, Inc., Knoxville, Tennessee under the supervision of Bill Longmeyer.

C. Syntheses

1. Preparation of μ-Dithiobis(tricarbonyliron)

$Fe_2S_2(CO)_6$ was prepared by the method described by Hieber and Gruber[40] as modified by Seyferth and co-workers.[41]

$$2Fe(CO)_4^{2-} + S_5^{2-} \xrightarrow{H^+} Fe_2S_2(CO)_6 + 3H_2S + 2CO + NaCl$$

Sodium polysulfide solution was prepared as follows: To a solution of 400 ml distilled H_2O and 100 g Na_2S, 55 g sublimed sulfur and 10 ml 50% aqueous KOH (w/v) were added. After the solution was allowed to stir until most of the sulfur dissolved, the solution was filtered and transferred to a 1000 ml side arm flask, degassed, and cooled to 0°C.

A 3000 ml, round-bottomed, three-necked flask equipped with a mechanical stirrer, gas-inlet tube, and a tight fitting serum stopper was charged with 200 ml degassed methanol and 35 ml filtered iron pentacarbonyl. After the vessel was cooled to 0°C and degassed several times, 80 ml of degassed 50% aqueous KOH (w/v) was added via cannula. To this solution, the Na_2S_5 solution was added as quickly as possible through a funnel, against a counter flow of nitrogen. During the addition, the mixture was vigorously stirred. A mildly exothermic reaction resulted with formation of a dark red solution. The reaction mixture was stirred at 0°C for two hours.

Cautious acidification of the reaction mixture was accomplished by slow addition of ∿400 ml 6 M HCl from an addition funnel. Evolution of hydrogen sulfide and carbon monoxide resulted, and a brown precipitate and colorless solution were formed. After filtration, the brown solid was air dried and divided into three portions. Each portion was extracted with hexanes until no color was present in the extraction solution. The combined extracts were evaporated on a rotary evaporator. A reddish semi-crystalline product containing a mixture of $FeS_2(CO)_6$ and $Fe_3S_2(CO)_9$ resulted. Sublimation at 40°C (0.1 mm pressure) overnight yielded 5-10 g of pure, ruby-red, air-stable crystals (12-24%, based on $Fe(CO)_5$), m.p. 46-47°C (lit.[40] 46.5°C), I.R. (MeCN solution): 2085 s, 2044 vs, and 2006 vs cm^{-1} (lit.[42] 2081, 2038, 1996 cm^{-1}).

2. Preparation of $(BzEt_3N)_2[MoFe_6S_6(CO)_{18}]$

$$Fe_2S_2(CO)_6 + 2LiEt_3BH \rightarrow Fe_2S_2(CO)_6^{2-} + Et_3B + H_2$$

$$3Fe_2S_2(CO)_6^{2-} + MoCl_5 \rightarrow [MoFe_6S_6(CO)_{18}]^{2-} + LiCl$$

$Fe_2S_2(CO)_6$ (1.2043 g; 3.50 mmole) was dissolved in 90 ml degassed tetrahydrofuran in a 300 ml Schlenck tube, and cooled to -78°C by using a Dry-Ice/isopropanol bath. Then 7.2 ml of 1.0 M $LiEt_3BH$ solution was added at a

rate of 0.5 ml per 5-10 min with use of a gas-tight syringe. In a 50 ml round-bottomed, side arm flask, $MoCl_5$ (0.3190 g; 1.168 mmole) was dissolved in 10 ml degassed acetonitrile. The resulting room-temperature solution was then added dropwise to the dianion solution at a rate of two drops per second, using a gas-tight syringe. After complete addition, the reaction mixture was slowly allowed to warm to room temperature. To this, $(BzEt_3N)Cl$ (0.5845 g; 2.45 mmole) dissolved in 30 ml MeCN was added. The resulting solution was stirred for one hour, filtered to remove LiCl, and the filtrate was evaporated in vacuo to approximately half the original volume and slowly cooled to -20°C in a freezer. Filtration at 0°C resulted in ∿50 mg crystalline purple by-product. The filtrate was then evaporated in vacuo at room-temperature to ∿20 ml, after which 20 ml degassed isopropanol was added dropwise via cannula. After slowly cooling the solution to -20°C and allowing it to remain undisturbed for two days, the mixture was filtered at 0°C, resulting in 350 mg crystalline product. The product was recrystallized by dissolving in 20 ml of 50% MeCN in THF, slowly adding 10 ml isopropanol, and cooling to -20°C for three days. This resulted in collection of 200 mg pure crystalline product (11.3% yield). Anal. Calcd for $(BzEt_3N)_2[MoFe_6S_6(CO)_{18}]$: C, 34.93; H, 2.91; N, 1.85; S, 12.73; Fe, 22.17; Mo, 6.35. Found: C, 34.95; H, 3.55; N, 2.12; S, 14.01; Fe, 22.04; Mo, 6.78. IR (MeCN

solution): 2070, 2037, 1990 cm^{-1}. Optical spectrum: 327, 459, 572 (sh) and 668 (sh) nm.

3. Preparation of $[Ph_3PCH_2CH_2PPh_3][MoFe_6S_6(CO)_{18}]$

The procedure was the same as described for the benzyltriethylammonium salt except for the work up, which was changed due to the different solubility characteristics of this salt.

After the addition of $[Ph_3PCH_2CH_2PPh_3]Br_2$ (0.71 g, 1.28 mmole), the mixture was evaporated *in vacuo* to dryness and redissolved in a minimum amount of EtCN. Et_2O was added dropwise until no further precipitation of LiCl/LiBr was noticed. After filtration and addition of an additional 5-10 ml Et_2O, the solution was cooled to -20°C, whereupon crystalline product separated in ~20% yield. Recrystallization was accomplished from EtCN/Et_2O. The product was isolated as dark needles in 15% yield. Anal. Calcd for $[Ph_3PCH_2CH_2PPh_3][MoFe_6S_6(CO)_{18}]$: C, 40.03; H, 2.04; P, 3.69; S, 11.45; Fe, 19.94; Mo, 5.71. Found: C, 42.41; H, 2.78; P, 3.88; S, 12.83; Fe, 19.63; Mo, 6.90. IR and optical spectra are identical with those of the benzyltriethylammonium salt.

III. RESULTS AND DISCUSSION

A. Synthesis

The compound was formed by reaction of three equivalents $[Fe_2S_2(CO)_6]^{2-}$ with one equivalent molybdenum pentachloride in tetrahydrofuran solution. After undergoing a metathesis reaction and upon concentration of the solution, the compound was isolated as either the $BzEt_3N^+$ or $(Ph_3PCH_2CH_2PPh_3)^{2+}$ salt.

The stoichiometry of the compound was determined by elemental analyses of the two isolated salts. The composition percentages found agreed with those calculated for the proposed formulation: $[MoFe_6S_6(CO)_{18}]$, see Table I. Furthermore, by comparing the %P or %N in the respective salt, it was found that either one $(Ph_3PCH_2CH_2PPh_3)^{2+}$ cation or two $(BzEt_3N)^+$ cations were present. When taking this into consideration, the compound must be a dianion with the postulated formulation of $[MoFe_6S_6(CO)_{18}]^{2-}$.

The synthesis of $[MoFe_6S_6(CO)_{18}]^{2-}$ from molybdenum pentachloride and dithiobis)tricarbonyliron) dianion, Figure IV, can be viewed as a combination oxidation-reduction and ligand-exchange reaction. The molybdenum is reduced from Mo(V) to Mo(IV) with some of the dianion

Table I. Elemental Analyses Data for the 1,2-Ethylenebis-(triphenylphosphonium) and Benzyltriethylammonium salts of $[MoFe_6S_6(CO)_{18}]^{2-}$.

$(Ph_3PCH_2CH_2PPH_3)^{2+}$	%C	% H	% P	% S	% Fe	% Mo
Calculated:	40.03	2.04	3.69	11.45	19.94	5.71
Sample 1	40.05	2.69	4.31	11.05	17.18	4.82
Sample 2	42.41	2.78	3.88	12.83	19.63	6.90

$(BzEt_3N)^{+}$	%C	% H	% N	% S	% Fe	% Mo
Calculated	34.93	2.91	1.85	12.73	22.17	6.35
Sample 1	34.95	3.43	2.25	12.88	21.94	6.44
Sample 2	34.95	3.55	2.12	12.88	22.04	6.78

Figure IV. Reaction scheme for the formation of $[MoFe_6S_6(CO)_{18}]^{2-}$. Generation of $Fe_2S_2(CO)_6^{2-}$ was accomplished with $LiEt_3BH$, after which one equivalent of molybdenum pentachloride was added to every three equivalents of $Fe_2S_2(CO)_6^{2-}$.

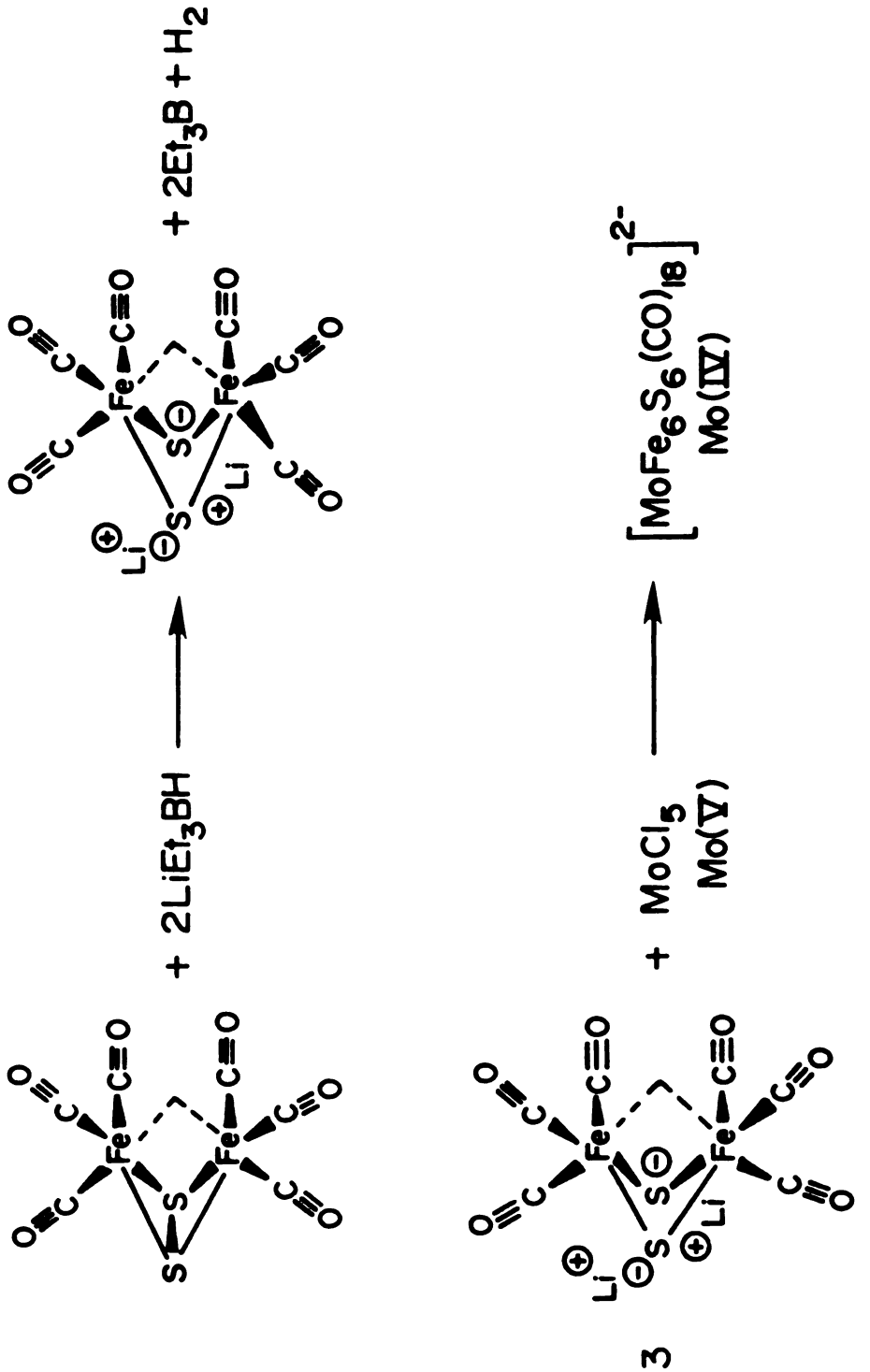

Figure IV

presumably being oxidized to its precursor, $Fe_2S_2(CO)_6$, or to some other unidentified iron-sulfur compound. Three $[Fe_2S_2(CO)_6]^{2-}$ units replace all the chlorides and coordinate to the molybdenum forming an octahedral sulfur environment around the molybdenum. The exact mechanism has not yet been established.

Since $[Fe_2S_2(CO)_6]^{2-}$ is thermally unstable, it is necessary to generate the dianion at -78°C. Tetrahydrofuran was found to be a suitable solvent, since it does not freeze at this low temperature and it is unreactive to the dianion. Unfortunately, molybdenum pentachloride is unstable in tetrahydrofuran,[43] producing the unwanted $MoOCl_3$ complex; so it is therefore necessary to use acetonitrile as solvent. Since the molybdenum pentachloride will also react with acetonitrile after several hours to afford the $MoCl_4(MeCN)_2$ complex,[44] it is necessary to minimize the time that the molybdenum pentachloride is left in solution. Also, since the dianion is decomposed by acetonitrile only a minimum amount can be used.

Upon addition of the molybdenum pentachloride/acetonitrile solution to the $[Fe_2S_2(CO)_6]^{2-}$/tetrahydrofuran solution, the dissolved molybdenum pentachloride reacts rapidly with the dithiobis(tricarbonyliron) dianion at -78°C, thus limiting the amount of decomposition by tetrahydrofuran. It is not unreasonable to suspect some decomposition which may be reflected in the low yield (~11%).

If the corresponding $MoOCl_3$ is formed in some minute amount, the formation of an iron-sulfur-molybdenyl complex should result. The formation of the purple complex, as described in the experimental section, can be explained as a formation of an iron-sulfur compound from the dithiobis(tricarbonyliron) dianion. This purple complex has been reproduced from other reactions[45] not containing molybdenum. This compound has not yet been characterized, but single crystals have been obtained in an extremely low yield; a crystal structure determination is in progress.

In the corresponding reaction using molybdenum tetrachloride, no pure products were isolated. The infrared spectrum of the reaction mixture showed a large number of bands in the carbonyl region, which suggests the formation of a mixture of compounds that could not be separated by crystallization with the quaternary cation salts (Et_4N^+, Bu_4N^+, Ph_4As^+, PPN^+, $(Ph_3PCH_2CH_2PPh_3)^{2+}$, $BzEt_3N^+$) used.

The $[MoFe_6S_6(CO)_{18}]^{2-}$ cluster has been isolated as various quaternary salts, including Bu_4N^+, $BzEt_3N^+$, $(Ph_3PCH_2CH_2PPh_3)^{2+}$, and Ph_4As^+. Single crystals of the $(Ph_3PCH_2CH_2PPh_3)^{2+}$ and $BzEt_3N^+$ salts have been obtained.

B. Solution Conductivity

By comparison of solution conductance measurements, it has been shown[44,46] that the magnitude of conductivity falls into ranges depending on the number of ions in

solution. Thus, separate ranges are generally found for 1:1, 2:1, and 3:1 electrolytes. This neglects the formation of ion pairs,[47] which frequently occurs in some low dielectric constant solvents. If this does occur, a substantially low conductivity reading will be observed, usually well below the expected value.

Solution conductivity measurements were performed on two different salts of the $[MoFe_6S_6(CO)_{18}]^{2-}$ complex, and compared to several 1:1 and 2:1 electrolytes. These were performed on acetonitrile solutions with electrolyte concentrations of 3.0×10^{-3} and 1.5×10^{-3} M. Relevant data are given in Table II.

For 3.0×10^{-3} M solutions of known 1:1 and 2:1 electrolytes, the ranges of 3.85-2.39 x 100 micromhos and 6.34-4.57 x 100 micromhos were found, respectively. Conductivity measurements for 3.0×10^{-3} M solutions of the 1,2-ethylenebis(triphenylphosphonium) and benzyltriethylammonium salts of the compound gave readings of 2.34 x 100 micromhos and 4.34 x 100 micromhos, respectively. These values fall on or slightly below the low end of the 1:1 and 2:1 electrolyte ranges, as might be expected given the likely size and consequent relatively low mobility of the proposed dianion.

Assuming that there is no ion pairing, this experiment suggests evidence that the complex is indeed a dianion in solution, thus supporting the formulation of the compound

Table II. Solution Conductivity Data Obtained in Acetonitrile.

Electrolyte Type	Salt Name	Concentration	Conductivity (×100 Micromhos)
1:1	$[Bu_4N][ClO_4]$	3×10^{-3} M	3.33
		1.5×10^{-3} M	1.75
	Et_4NCl	3×10^{-3} M	3.85
		1.5×10^{-3} M	2.03
	$[Bu_4N][Ph_4B]$	3×10^{-3} M	2.39
		1.5×10^{-3} M	1.24
1:2	$[Ph_3PCH_2CH_2PPh_3](PF_6)_2$	3×10^{-3} M	6.34
		1.5×10^{-3} M	3.42
2:1	$[Et_4N]_2MoS_4$	3×10^{-3} M	4.60
		1.5×10^{-3} M	2.58
1:2	$[Ph_3PCH_2CH_2PPh_3]Br_2$	3×10^{-3} M	4.57
		1.5×10^{-3} M	2.57
1:3	$[Cr(en)_3](Ph_4B)_3$	3×10^{-3} M	2.29*
		1.5×10^{-3} M	1.30*
	$[PhPCH_2CH_2PPh_3][MoFe_6S_6(CO)_{18}]$	3×10^{-3} M	2.34
		1.5×10^{-3} M	1.41
	$[BzEt_3N]_2[MoFe_6S_6(CO)_{18}]$	3×10^{-3} M	4.34
		1.5×10^{-3} M	2.43

*Substantial ion pairing present.

as being a monomeric unit with the oxidation state of the molybdenum being +4.

C. Infrared Spectroscopy

Infrared spectroscopy has been used primarily as a qualitative method for examining product purity. The pure product showed three well resolved bands in the carbonyl stretching region, while the crude semi-crystalline material isolated from the reaction mixture showed the presence of additional bands which were not as well defined. All spectra were taken in solution, usually acetonitrile or propionitrile, with a NaCl IR solution cell adapted with tight fitting serum caps.

The infrared spectrum of $[MoFe_6S_6(CO)_{18}]^{2-}$ in the region of 2000 cm^{-1} represents C-O stretching modes. Three bands were observed at 2070, 2037, and 1990 cm^{-1}, as shown in Figure V.

In dithiobis(tricarbonyliron) three infrared active bands are observed at 2081, 2038, and 1996 cm^{-1}, as reported by Hieber and Beck,[42] see Figure V. Assignment of all infrared and Raman active bands to their respective modes in dithiobis(tricarbonyliron) was accomplished by Scovell and Spiro.[48]

Since there are only three carbonyl stretching frequencies present in the infrared spectrum of the $[MoFe_6S_6(CO)_{18}]^{2-}$ cluster, the same number that is present in the infrared spectrum of $Fe_2S_2(CO)_6$, suggests evidence that there

Figure V. Infrared spectra of $[MoFe_6S_6(CO)_{18}]^{2-}$, (top), and $Fe_2S_2(CO)_6$ in acetonitrile at 20°C. Calibrated with polystyrene film.

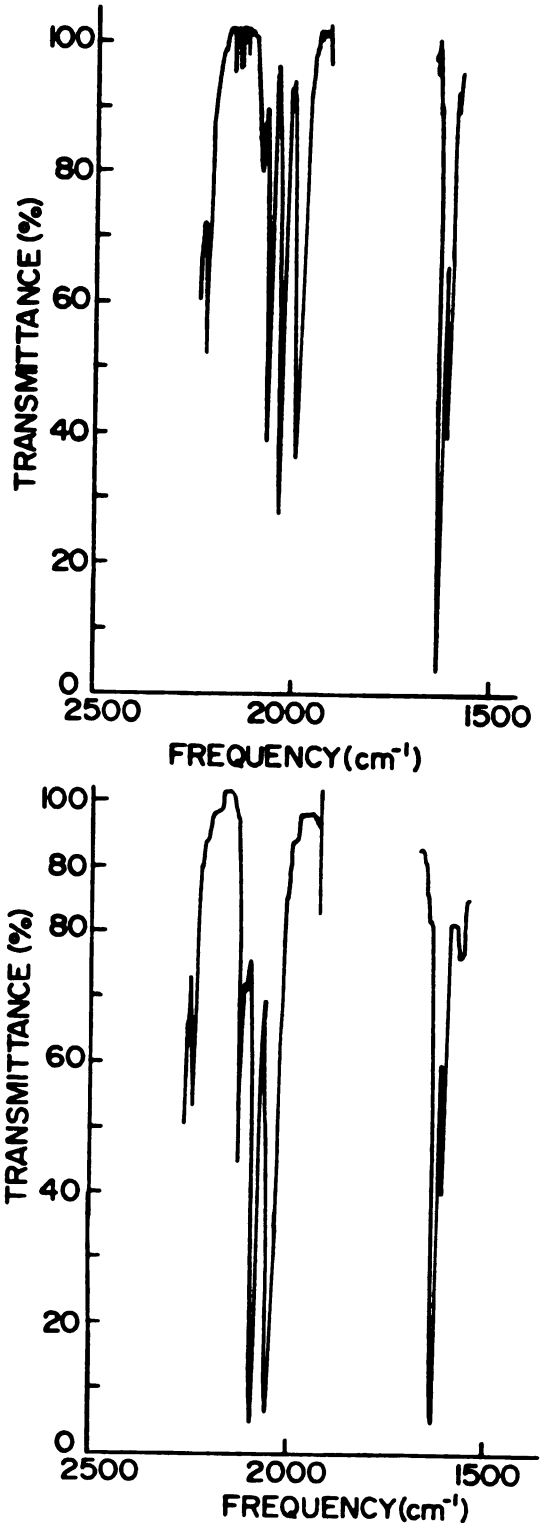
100
80
60
40
20
0
TRANSMITTANCE (%)
2500
2000
1500
FREQUENCY(cm⁻¹)
100
80
60
40
20
0
TRANSMITTANCE (%)
2500
2000
1500
FREQUENCY(cm⁻¹)

Figure V

are three individual dimer units present in an arrangement where their vibrations are not strongly coupled.

Upon comparison of the three carbonyl stretching frequencies given for $Fe_2S_2(CO)_6$, $[Fe_2S_2(CO)_6]^{2-}$, and $[MoFe_6S_6(CO)_{18}]^{2-}$, see Table III, an interesting trend was observed.

When $Fe_2S_2(CO)_6$ is reduced to $[Fe_2S_2(CO)_6]^{2-}$, the net negative charge on the sulfur is transmitted inductively to the iron, thus increasing the extent of back-donation from the iron to the carbonyls. This in turn, increases the Fe-C bond strength and decreases the $C \equiv O$ bond strength, resulting in a downward shift of the carbonyl stretching frequencies.

After coordination of the $[Fe_2S_2(CO)_6]^{2-}$ units to the molybdenum, some of this negative charge is withdrawn from the sulfur to the molybdenum, thus reducing the amount of charge transmitted to the iron. This decreases some of the back-donation from the iron to the carbonyls, causing a slight decrease in Fe-C bond strength and a slight increase in $C \equiv O$ bond strength, resulting in an upward shift in the carbonyl stretching frequencies.

Further detailed studies employing infrared and Raman spectroscopy would be necessary to examine the other vibrations in the molecule.

Table III. Infrared Spectroscopic Data in Carbonyl Stretching Region.

Compound	Frequency (cm^{-1})
$Fe_2S_2(CO)_6$	2081
	2038
	1996
*$[Fe_2S_2(CO)_6]^{2-}$	2025
	1975
	1945
$[MoFe_6S_6(CO)_{18}]^{2-}$	2070
	2037
	1990

*Since this compound is thermally unstable, these frequencies may be incorrect.

D. Electronic Spectroscopy

The optical spectrum of $[MoFe_6S_6(CO)_{18}]^{2-}$ is shown in Figure VI, and pertinent data are presented in Table IV.

Due to the high molar extinction coefficients of all the observed peaks, they must be ligand to metal charge transfer in nature rather than d-d transitions. Unfortunately, the spectra of only a few non-oxo, six coordinate molybdenum (IV) compounds have been reported; a survey of these is given in Table V. All of these molybdenum (IV) complexes exhibit very intense bands in the region of 250-550 nm with molar extinction coefficients of $\sim$5-16 x 10^3 M^{-1} cm^{-1}. These have been assigned as L $\rightarrow$ Mo charge transfer transitions.

Therefore, the intense absorptions at 327 nm ($\varepsilon \simeq$ 37000 M^{-1} cm^{-1}) and 459 nm ($\varepsilon \simeq$ 9700 M^{-1} cm^{-1}) can be assigned as S $\rightarrow$ M (M = Mo or Fe) charge-transfer transitions. Similar absorptions with high molar extinction coefficients in the 300-500 nm region were observed in other molybdenum-iron-sulfur clusters,[31-37] in which the charge-transfer transitions were assigned to S $\rightarrow$ M (Mo or Fe). At this point, it is not possible to differentiate between S $\rightarrow$ Mo and S $\rightarrow$ Fe transitions, although the absence of the band at $\sim$450 nm in $Fe_2S_2(CO)_6$ and $Fe_2S_2(CO)_6^{2-}$ suggests that the 459 nm peak is probably due to an S $\rightarrow$ Mo charge-transfer transition.

Assignment of the two weak shoulders at 572 nm

Figure VI. Optical spectra of $[MoFe_6S_6(CO)_{18}]^{2-}$ (solid line), and $Fe_2S_2(CO)_6$ in acetonitrile solution at 20°C.

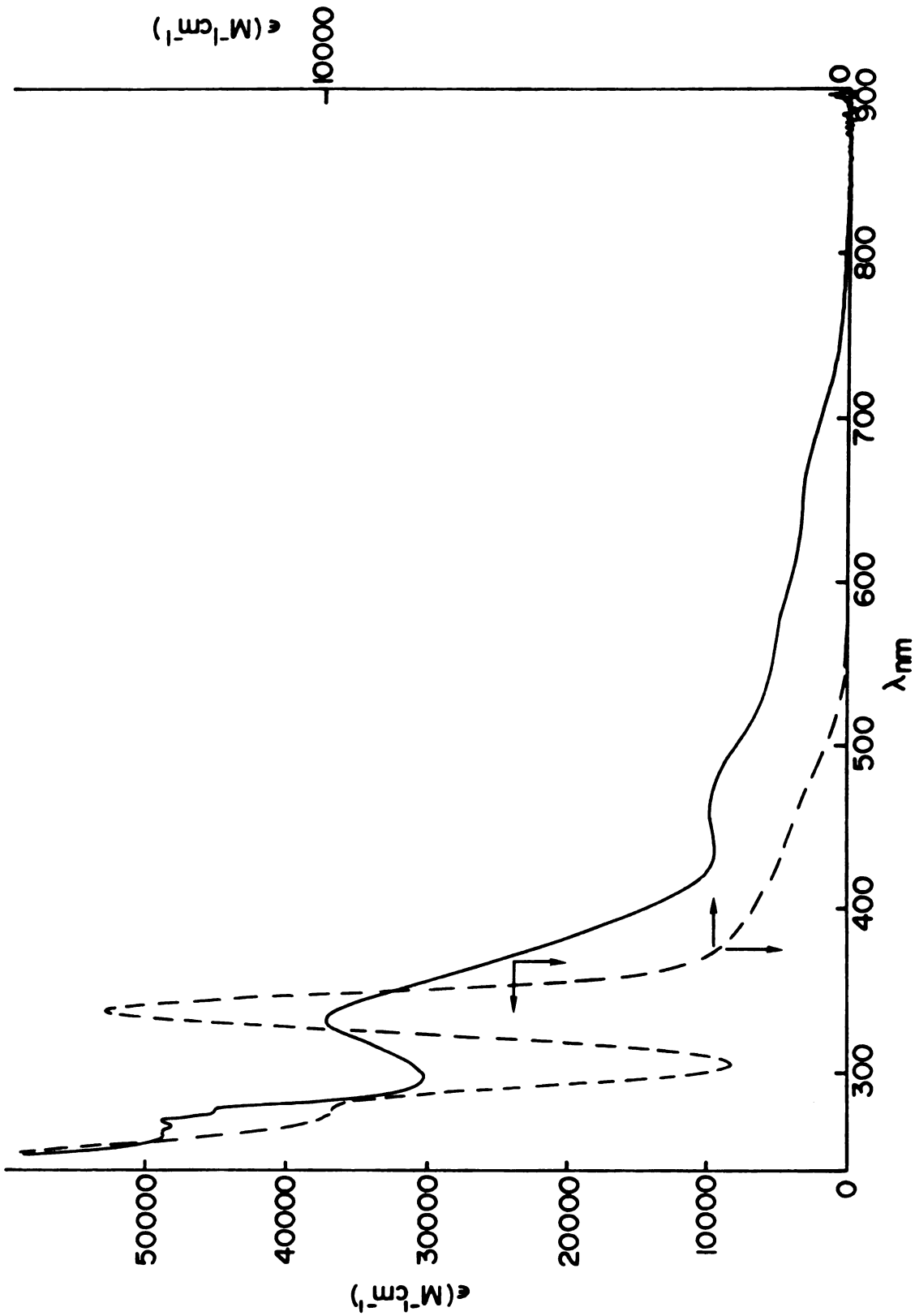
ε(M⁻¹cm⁻¹)
50000
40000
30000
20000
10000
0
300
400
500
600
700
800
900
λnm
ε(M⁻¹cm⁻¹)
10000

Figure VI

Table IV. Electronic Spectroscopic Data.

Compound	Peak (nm)	Extinction Coefficient (ℓ mole^{-1} cm^{-1})
$[MoFe_6S_6(CO)_{18}]^{2-}$	327	37,000
	459	9,700
	572 (sh)	4,900
	668 (sh)	2,900
$Fe_2S_2(CO)_6$	278 (sh)	8,800
	333	14,000
	450 (sh)	1,000
*$Fe_2S_2(CO)_6^{2-}$	330	---
	430 (sh)	---
	580	---

*Since this compound is thermally unstable, these absorptions may be incorrect.

Table V. Absorption Spectra of Some Non-oxo, Six Coordinate Molybdenum (IV) Complexes.

Compound	Peak λ_{nm}	Extinction Coefficient	Assignment	Ref.
$MoCl_6^{2-}$	242		CT	50
	272		CT	
	294		CT	
	352		CT	
	387		d-d	
	450		d-d	
$MoCl_4(dipy)$	239	14000	CT $\pi \rightarrow \pi^*$	51
	302	12000	CT $\pi \rightarrow \pi^*$	
	368	1200	CT	
	397	800	d-d	
	546	690	d-d	
$MoCl_4(MeCN)_2$	240	3000	CT	44
	285	2400	CT	
	314	2900	CT	
	359	~900	CT?	
	400	~400	CT?	
	495	75	d-d	
$Mo(sal\text{-}NEt)_2Cl_2$*	352	15290	CT	52
	430	4360	CT	
	550	5810	CT	

*Sal = N-substituted salicylalimiato.

($\varepsilon \simeq 4900\ M^{-1}\ cm^{-1}$) and 668 nm ($\varepsilon \simeq 2900\ M^{-1}\ cm^{-1}$) can be only speculative. Their molar extinction coefficients are again too high to be d-d transitions, so they must be due to charge-transfer. The energies of these transitions are different from the usual high energy bands seen in molybdenum-iron-sulfur clusters. This energy difference may be interpreted by examination of the σ and π symmetry of the bonding orbitals within the complex. This allows both $S\sigma \rightarrow M$ and $S\pi \rightarrow M$ charge-transfer transitions with differing energies.

Most pseudo-octahedral molybdenum (IV) complexes exhibit two peaks in the visible region above 400 nm, which have been tentatively assigned to the d-d transitions: $^3T_{2g} \leftarrow {}^3T_{1g}$ and $^3T_{1g}(P) \leftarrow {}^3T_{1g}$.[49] These peaks usually have molar extinction coefficients well below $1000\ M^{-1}\ cm^{-1}$.[44,51] It is a reasonable assumption that these d-d transitions are obscured by the lower energy charge-transfer transitions at 668 nm and 572 nm.

E. Mössbauer Spectroscopy

The ^{57}Fe Mössbauer spectrum of $[MoFe_6S_6(CO)_{18}]^{2-}$ has given useful insight towards the structure of this complex. In the proposed structure, all of the iron atoms are equivalent with each having the formal oxidation state of +1. The expected ^{57}Fe Mössbauer spectrum would consist of a doublet with an isomer shift and quadrupole splitting

near the values obtained for Fe(I) in other related compounds.

A correlation diagram for ^{57}Fe Mössbauer is shown in Figure VII, in which isomer shift ranges are drawn as a function of oxidation state.[53] The isomer shift ranges for the different oxidation states in ionic iron compounds seldom overlap one another, so it is therefore relatively easy to determine the oxidation state of the iron in unknown iron compounds.

The ^{57}Fe Mössbauer spectrum of $[MoFe_6S_6(CO)_{18}]^{2-}$ at 4.2 K is presented in Figure VIII. A doublet was observed with E_Q = 0.80 mm/sec and δ = 0.06 mm/sec.

With comparison to the spectra of $Fe_2S_2(CO)_6$ shown in Figure IX, and other compounds, Table VI, the isomer shift and quadrupole splitting values are in good agreement with those of similar Fe(I) compounds.

Since no magnetic hyperfine interactions were observed, probably due to rapid electronic relaxation in the solid plus an integral spin ground state, nothing else can be determined except that all the iron atoms have the formal oxidation state of +1 and they are arranged so that they are all equivalent.

Figure VII. Approximate ranges of isomer shifts observed in iron compounds relative to metallic iron at room temperature. S refers to the spin quantum number.

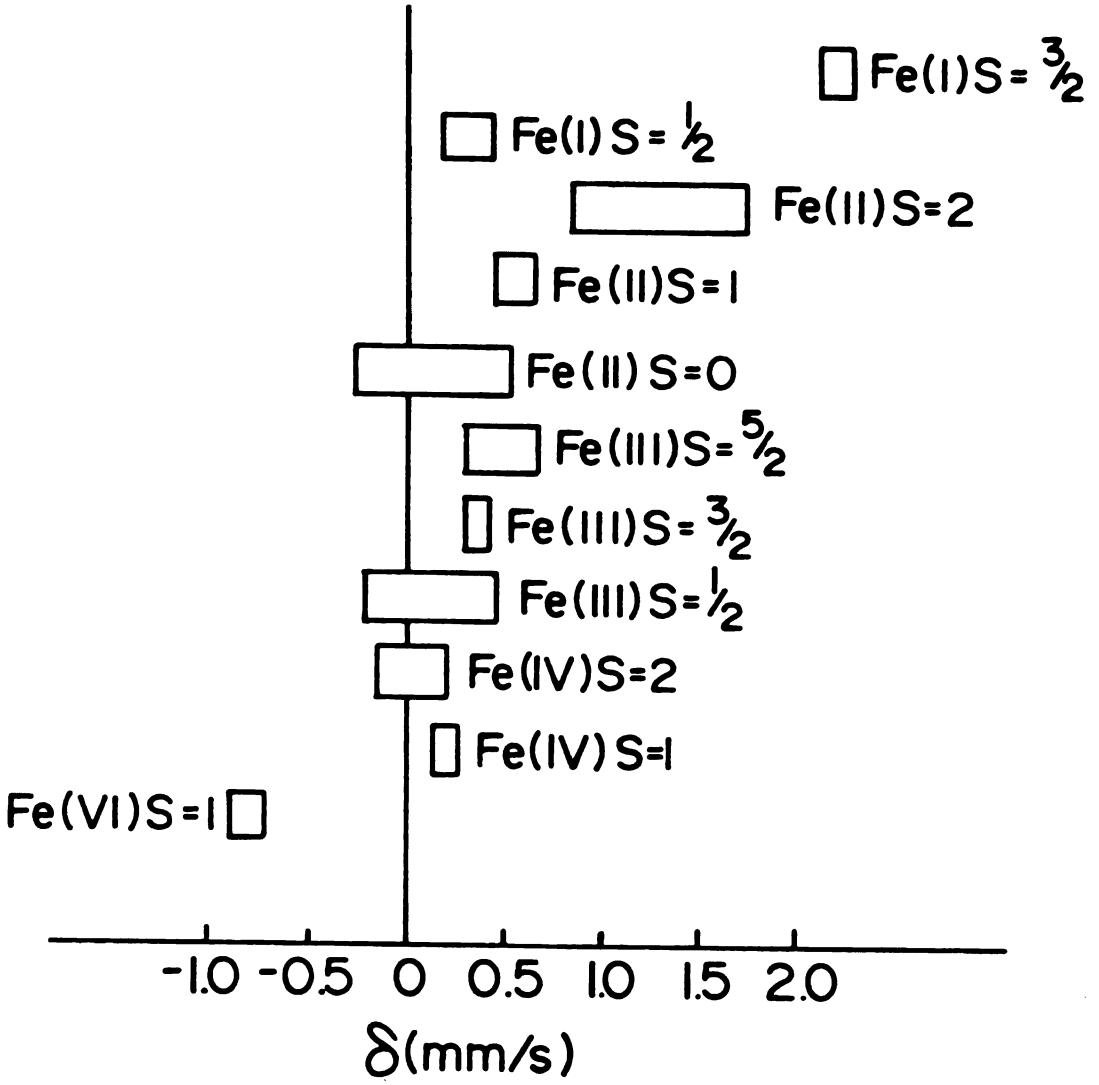
Fe(I)S= 3/2
Fe(I) S= 1/2
Fe(II)S=2
Fe(II)S=1
Fe(II) S=0
Fe(III)S= 5/2
Fe(III)S= 3/2
Fe(III)S= 1/2
Fe(IV)S=2
Fe(IV) S=1
Fe(VI)S=1
-1.0 -0.5 0 0.5 1.0 1.5 2.0
δ(mm/s)

Figure VII

Figure VIII. Mössbauer spectrum of $[MoFe_6S_6(CO)_{18}]^{2-}$ as a polycrystalline sample diluted with boron nitride. Recorded at 4.2 K with a 600 G magnetic field.

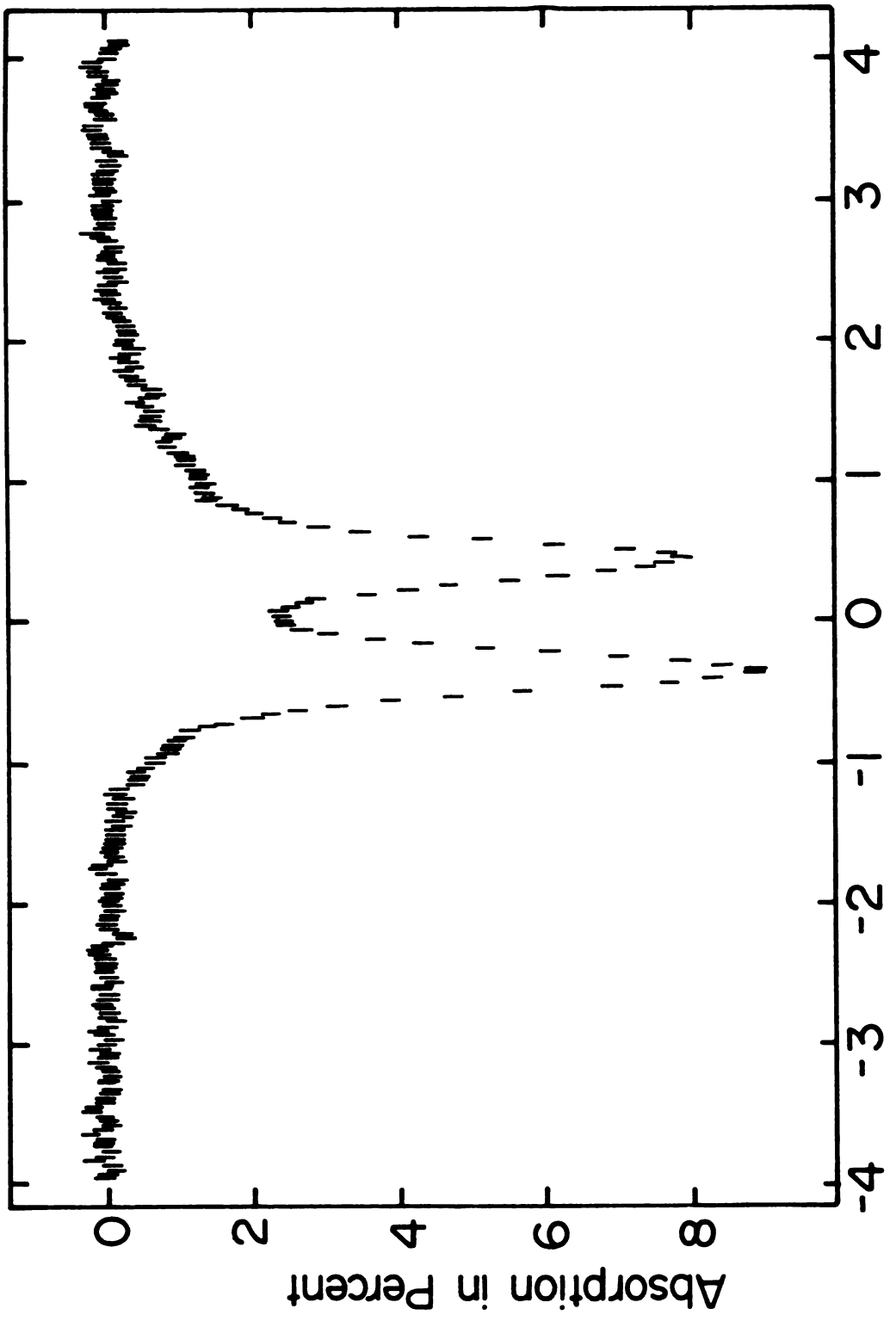

Figure VIII

Figure IX. Mössbauer spectrum of $Fe_2S_2(CO)_6$ as a polycrystalline sample diluted with boron nitride. Recorded at 4.2 K with a 600 G magnetic field.

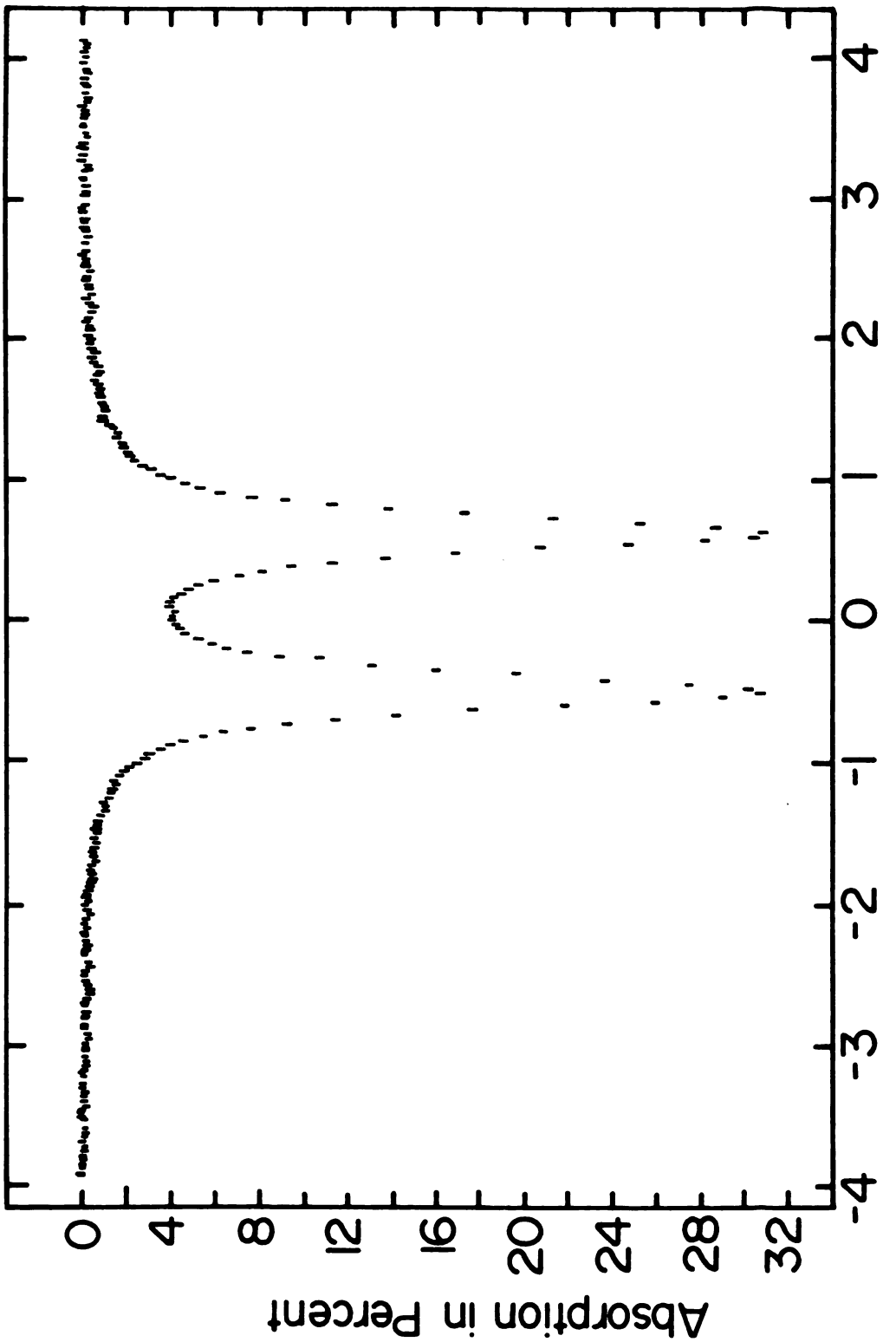
Absorption in Percent
0
4
8
12
16
20
24
28
32
-4
-3
-2
-1
0
1
2
3
4
Velocity in mm/s

Figure IX

Table VI. Mössbauer Data for $[MoFe_6S_6(CO)_{18}]^{2-}$, $Fe_2S_2(CO)_6$, and Other Iron Compounds.

Compound	δ(mm/s)	ΔE_Q (mm/s)	Remarks	Ref.
$(BzEt_3N)_2[MoFe_6S_6(CO)_{18}]$	0.06	0.80	4.2 K, 600 G	--
$Fe_2S_2(CO)_6$	0.08	1.11	4.2 K, 600 G	--
$(CO)_3Fe(SPh)_2Fe(CO)_3$	0.061	1.067	80 K	54
cis-$(CO)_3Fe(SMe)_2Fe(CO)_3$	0.29	0.895	80 K	54
$Fe(CO)_5$	0.085	2.57	78 K	55
$[Fe_2S_2(S_2\text{-o-xyl})_2]^{2-}$	0.17			56
$[Fe_4S_4(SPh)_4]^{2-}$	0.35			57
$[Fe(SPh)_4]^{2-}$	0.64			58

F. Magnetic Susceptibility

The room temperature magnetic susceptibility of $[MoFe_6S_6(CO)_{18}]^{2-}$ has been determined by the Faraday method. The data gave rise to an effective magnetic moment of 4.85 BM, after corrections for diamagnetic contributions to the susceptibility from the ligands and cations by use of Pascal's constants. This effective magnetic moment is significantly larger than the spin-only value (μ_{eff} = 2.83 BM) expected for two unpaired electrons in an S = 1 ground state.

If we assume that the large magnetic moment is due to a paramagnetic impurity, such as high-spin Fe(III), a contribution to the molar susceptibility of 1.72×10^{-3} $EMU \cdot M^{-1}$ would be necessary to achieve the observed value of 4.85 BM. This would correspond to ~15% of the total iron being present as high-spin Fe(III). If this were the case, an additional quadrupole doublet in the ^{57}Fe Mössbauer spectrum would be expected, but was not observed.

Octahedral molybdenum (IV) has a $^3T_{1g}$ ground state; thus an orbital contribution is expected due to the orbitally degenerate triplet ground state. Since the environment around the molybdenum atom is highly symmetrical and an electron can occupy these degenerate orbitals, a circulation of the electron about the molybdenum is permitted, thus causing a large orbital contribution.

Molybdenum (IV) complexes have a d^2 electronic

configuration in which the shell is less than half full, thus the $\lambda L \cdot S$ factor is positive, thereby causing a negative contribution to the effective magnetic moment. Most pseudo-octahedral molybdenum (IV) compounds have moments ranging from 1.9 - 2.8 BM. Typical values reported in the literature include: K_2MoCl_6,[52] μ_{eff} = 2.28; $K_2Mo(NCS)_6$,[59] μ_{eff} = 3.02. If the $[MoFe_6S_6(CO)_{18}]^{2-}$ complex is considered as a simple pseudo-octahedral molybdenum (IV) compound, orbital contribution cannot explain the large magnetic moment.

A third possibility for an increase in the magnetic moment is that the compound may disproportionate to Mo(III) and Mo(IV) in the solid state. This has been observed in $(pyH)_2Mo(NCS)_6$,[60] (μ_{eff} = 2.45), in which after storing for a few months in sealed tubes gave rise to a magnetic moment of $\sim$3.5 BM. The other physical measurements, however, do not agree with disproportionation in the $[MoFe_6S_6(CO)_{18}]^{2-}$ complex.

Another possible contribution for the large moment may be due to temperature-independent-paramagnetism; which has been observed in one molybdenum (IV) complex: $MoO[py(anil)_2]Cl_2$,[60] (diamagnetic, μ_{eff} = 0.8 BM).

In order to examine the possibility that the large moment observed for $[MoFe_6S_6(CO)_{18}]^{2-}$ was due to an unusually large temperature-independent-paramagnetism, variable temperature

magnetic susceptibility measurements were taken. The temperature-dependent susceptibility data were found to conform to Curie-Law behavior, $\chi = C/(T + \theta)$, $c = 3.54$ EMU·K·M^{-1} and $\theta = -1.47$ K. The resulting plots of χ_m *vs* T and $1/\chi_m$ *vs* T are shown in Figures X and XI. In the plot of $1/\chi_m$ *vs* T, a slight downward trend is observed at higher temperatures. This trend is probably caused by a small contribution of temperature-independent-paramagnetism.[61] It seems likely that this contribution is not very large since the deviation from Curie-Law behavior is very small.

G. Electrochemistry

The electrochemical behavior of $[MoFe_6S_6(CO)_{18}]^{2-}$ was examined by using polarographic and cyclic voltammetric techniques. All measurements were made in acetonitrile solutions containing 1.5 mM $[MoFe_6S_6(CO)_{18}]^{2-}$ and 0.1 M $[Bu_4N][ClO_4]$ as supporting electrolyte. They were recorded relative to a standard calomel reference electrode.

The polarography techniques, employing a dropping mercury electrode, proved to be the most useful methods for studying the electrochemical behavior of this complex. Well-formed polarographic waves were obtained, which allowed reasonable assignments for the electrochemical data.

In cyclic voltammetry, a glassy carbon electrode was used instead of the more conventional platinum electrode. With platinum, the electrode surface was discolored after

Figure X. Magnetic susceptibility of $(BzEt_3N)_2[MoFe_6S_6(CO)_{18}]$ as a function of temperature in the solid state, obtained in a 2.000 kG magnetic field. Units for χ_m are $EMU \cdot M^{-1}$.

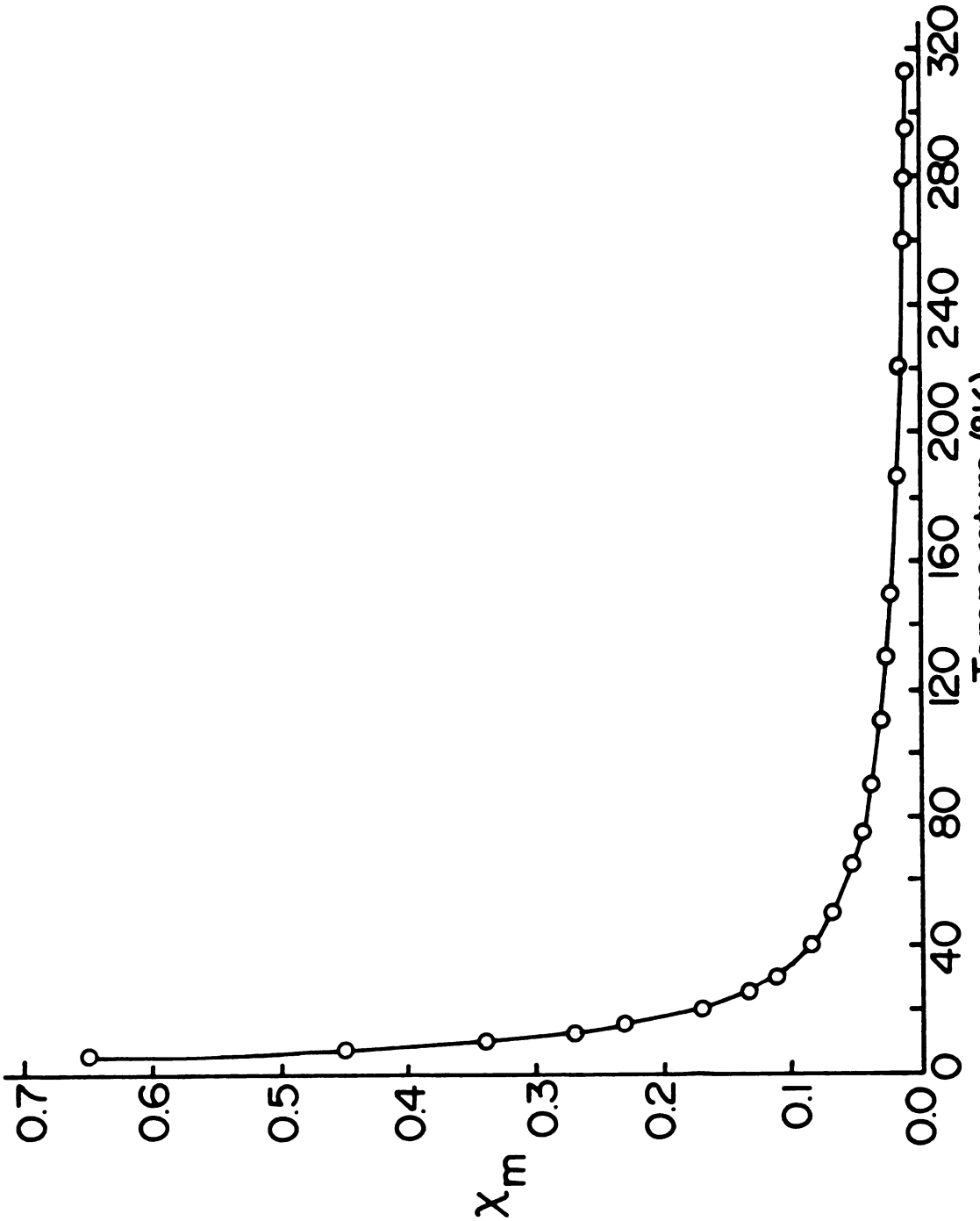
0.7
0.6
0.5
0.4
0.3
0.2
0.1
0.0
χ_m
0
40
80
120
160
200
240
280
320
Temperature (°K)

Figure X

Figure XI. Inverse of magnetic susceptibility of $(BzEt_3N)_2[MoFe_6S_6(CO)_{18}]$, $(M \cdot EMU^{-1})$, as a function of temperature. Slight downward slope is due to temperature-independent-paramagnetism. Obtained in a 2.000 kG magnetic field.

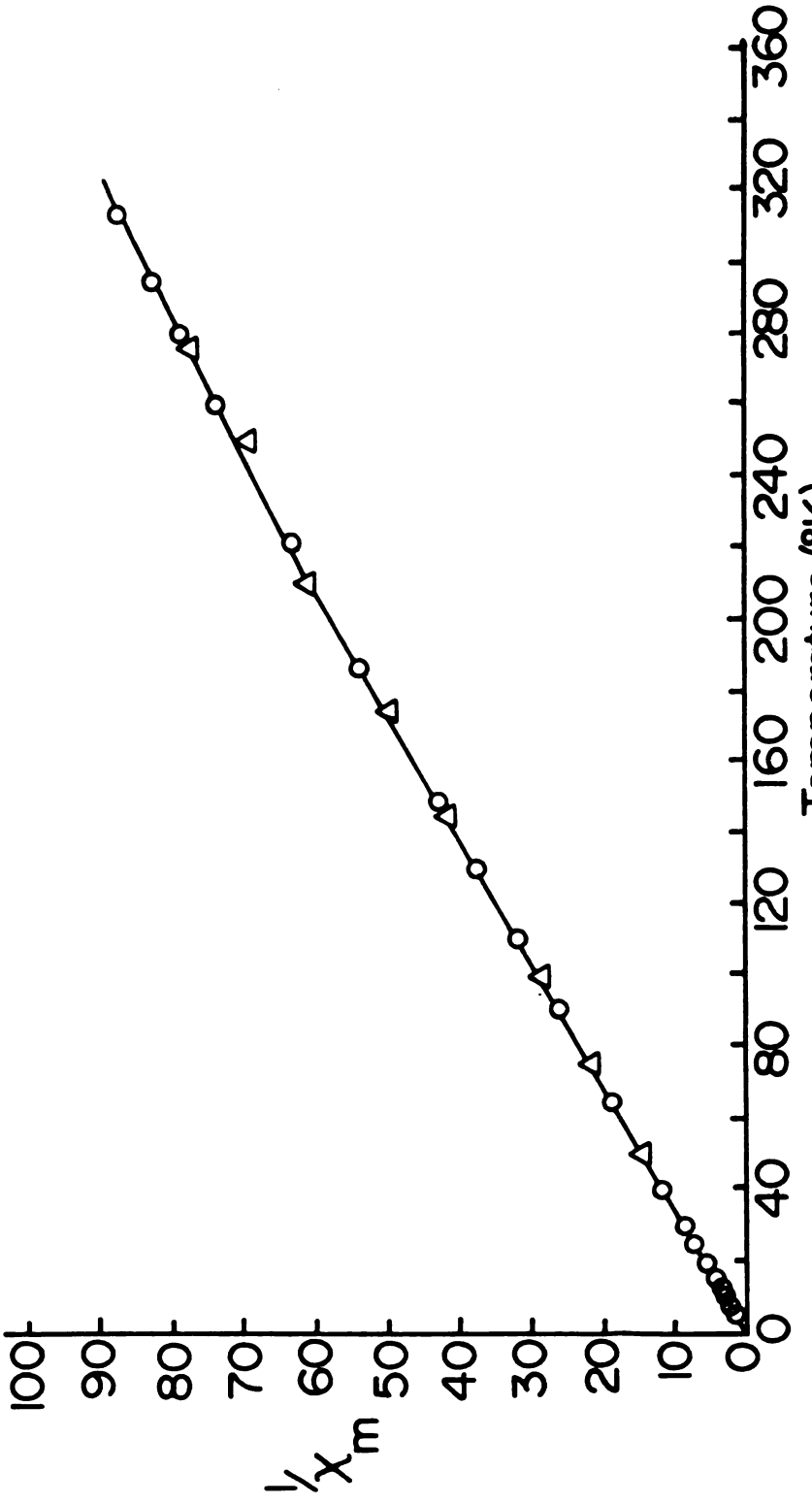
100
90
80
70
60
50
40
30
20
10
0
$1/\chi_m$
0
40
80
120
160
200
240
280
320
360
Temperature (°K)

Figure XI

a single scan due to problems associated with the adsorption of sulfur-rich complexes onto the platinum surface. Due to this adsorption problem, usually the cathodic wave was of reasonable shape and magnitude, but the anodic wave was featureless.

In using the glassy carbon electrode, several runs were necessary to condition the electrode surface, after which the waves became of a more reasonable shape. It was also necessary to clean the electrode surface prior to each scan.

It is not unreasonable to assume that the only reason the dropping mercury electrode system gave better results is due to the continual generation of a fresh electrode surface with each new drop.

Significant electrochemical data appear in Table VII. An example of a differential pulse polarogram for the first and second reductions is shown in Figure XII, and examples of cyclic voltammograms are shown for both the oxidation and first reduction processes in Figure XIII.

Examination of the electrochemistry of this complex over the potential range of 0.0 to -2.0 volts revealed two electrochemical reductions, the first of which is reversible. Plots of log $[i/(i_D-i)]$ *vs* voltage for the complex gave slopes near the theoretical value (59 mV) for a single, one-electron reversible reduction.

Since the value of the diffusion current (i_D) is

Table VII. Electrochemical Data for $[MoFe_6S_6(CO)_{18}]^{2-}$.

Solvent: MeCN Ref.: SCE	Polarography			Diff. Pulse Polarography		Cyc. Volt.		
	$E_{1/2}$ (V)	Slope (mV)	i d/c ($\frac{\mu A}{mM}$)	E_p (V)	$W_{1/2}$ (mV)	E (V)	$E_{pc}-E_{pa}$ (mV)	$\frac{i_{ap}}{i_{cp}}$
1st. red.								
$(Ph_3\overset{+}{P}CH_2CH_2\overset{+}{P}Ph_3)$	-1.194	-51.4	2.32	-1.217	-118	-1.198	-127	0.845
$BzEt_3N^+$	-1.198	-53.0	2.85	-1.223	-117	-1.182	-105	0.895
2nd. red.								
$(Ph_3\overset{+}{P}CH_2CH_2\overset{+}{P}Ph_3)$	-----	----	----	-1.780	---	-----	---	-----
$BzEt_3N^+$	-1.734	-51.4	7.97	-1.798	-130	-----	---	-----
Oxidation								
$(Ph_3\overset{+}{P}CH_2CH_2\overset{+}{P}Ph_3)$	-----	----	----	-----	---	+0.1306	+ 93	0.844
$BzEt_3N^+$	-----	----	----	-----	---	+0.1425	+123	0.759

			Process
1st. reduction	-1.196 V	reversible	2-/3-
2nd. reduction	-1.80 V	irreversible	
Oxidation	+0.137 V	reversible	2-/1-

Figure XII. Differential pulse polarogram of first and second electrochemical reductions of $[MoFe_6S_6(CO)_{18}]^{2-}$.

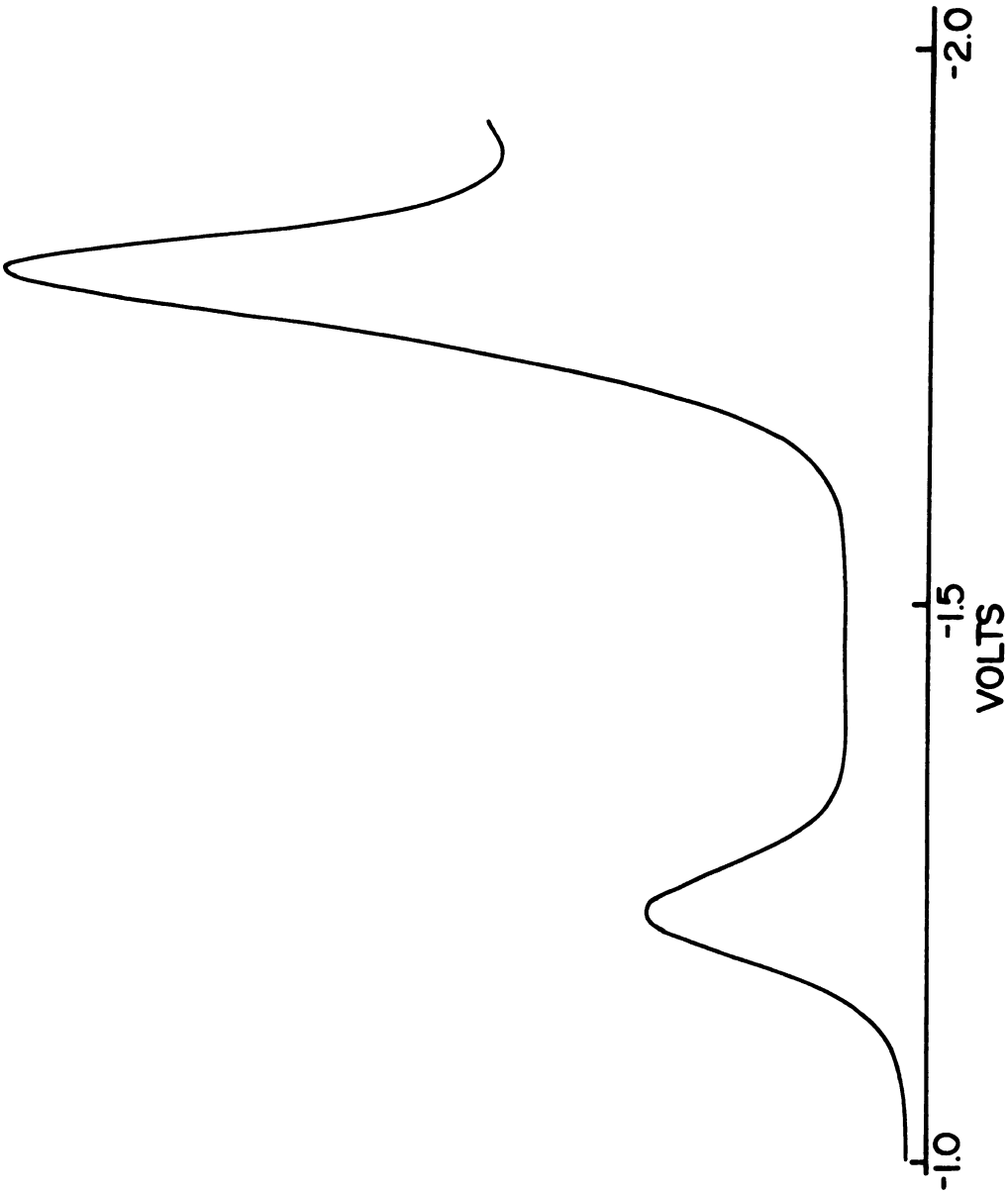

Figure XII

Figure XIII. Cyclic voltammograms of the first reduction process (top), and the oxidation process of $[MoFe_6S_6(CO)_{18}]^{2-}$. Scan rate: 100 mV/sec.

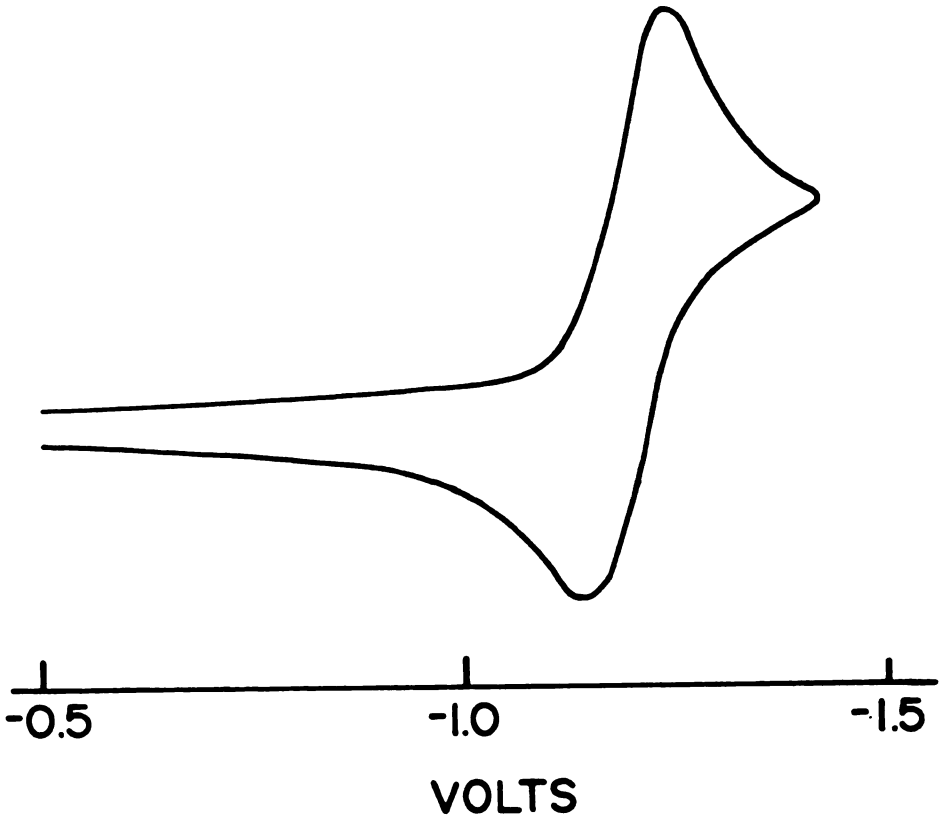

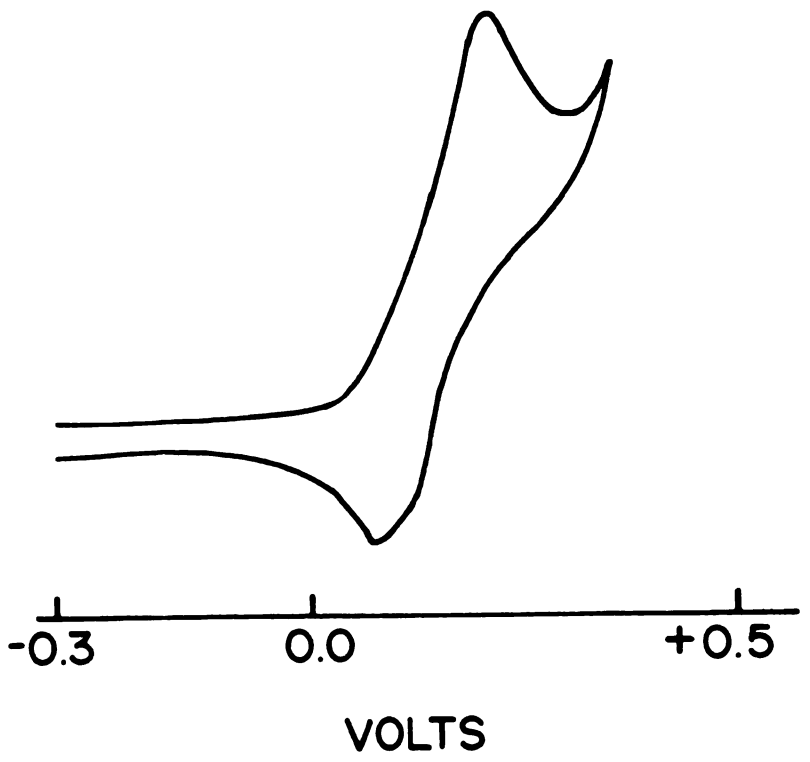

Figure XIII

dependent upon concentration of the complex ion, a relationship is observed when comparing the i_D values for other compounds, see Table II. The diffusion current value of the compound is near 2.5 μA/mM, which correlates well to that of the iron-sulfur tetramers ($i_D \approx 2.97$ μA/mM for SPh and $i_d \approx 2.45$ μA/mM for OPh). Since the tetramers have a 2-charge, this then also supports the formulation of $[MoFe_6S_6(CO)_{18}]^{2-}$ for the compound.

The reduction of the compound at -1.196 V is a reversible 2-/3- process. The reduction at -1.80 V was found to be due to a multi-electron process on the grounds of an extremely large i_D value (7.97 μA/mM).

In comparison to the reduction potentials for $Fe_2S_2(CO)_6$, see Table VIII, the potentials for the compound are very different as expected. The compound contains the $Fe_2S_2(CO)_6$ unit already reduced by two electrons as compared to the $Fe_2S_2(CO)_6$ itself.

With comparison to $[CH_3SFe(CO)_3]_2$, see Table VIII, a compound where the unit is reduced, it can be concluded that the 2nd reduction of the compound, (-1.80 V), may correlate to the first reduction of the $Fe_2S_2(CO)_6^{2-}$ unit (-1.9 V). The second reduction of the $Fe_2S_2(CO)_6^{2-}$ unit (-2.5 V) is well below any of the observed reduction potentials for the compound.

A quasi-reversible electrochemical oxidation was found at +0.137 V, which correlated to the 2-/1- process. These results suggest that it may be possible to isolate the 3- and possibly the 1- species.

Table VIII. Electrochemical Data for Other Compounds.

Compound	Solvent	Process	Slope (mV)	i_d (μA/mM)	Ref.
$[Fe_4S_4(SPh)_4]^{2-}$	MeCN	1st red	-62	2.97	63
		2nd red	-50	2.24	
$[Fe_4S_4(OPh)_4]^{2-}$	MeCN	1st red	-52	2.45	63
		2nd red	-50	2.75	

Compound	$E^1_{1/2}$ (V)	$E^2_{1/2}$ (V)	Ref.
$Fe_2S_2(CO)_6$	-0.49	-1.87 (ill defined)	
$[CH_3SFe(CO)_3]_2$	-1.9	-2.5 (ill defined)	64

H. X-ray Structural Studies

Excluding magnetic susceptibility measurements, all other evidence suggests the proposed structure shown schematically in Figure XIV. It has approximate D_{3d} symmetry with an octahedral sulfur environment around the molybdenum.

Attempts to isolate X-ray quality single crystals have met with little success. Different mono- and dication salts were used to try to achieve the best crystal size and shape. Only two different salts enabled the growth of reasonably sized single crystals. 1,2-Ethylenebis(triphenylphosphonium) gave needle like crystals, but contained severe surface defects and gave poor X-ray diffraction.

Benzyltriethylammonium yielded hexagonally shaped flat crystals which diffracted, but not well enough to allow collection of a complete data set.

It is possible that due to the almost spherical symmetry of the compound, the $MoFe_6S_6$ octahedra are disordered and randomly oriented within the crystal lattice. A possible solution to this problem is to remove the spherical symmetry by substitution of one or more of the carbonyls with another ligand, thus overcoming the disorder.

Phosphine ligands are known to react with $Fe_2S_2(CO)_6$[65] and undergo ligand exchange to afford the complexes $Fe_2S_2(CO)_5L$ and $Fe_2S_2(CO)_4L_2$ ($L = P(C_6H_5)_3$).

Initial experiments in which the $[MoFe_6S_6(CO)_{18}]^{2-}$

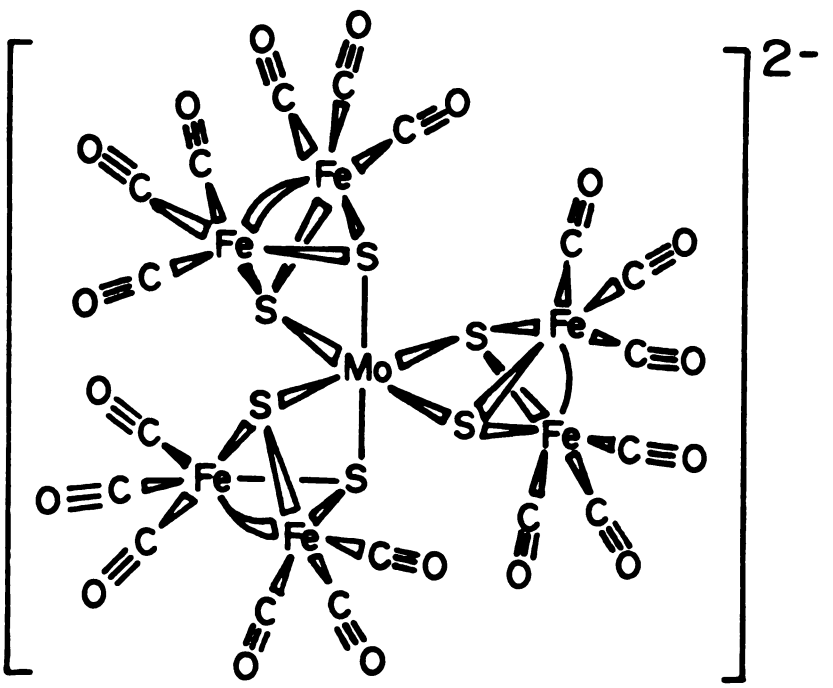

Figure XIV. Schematic representation of the proposed structure for $[MoFe_6S_6(CO)_{18}]^{2-}$. Compound has been isolated as $(BzEt_3N)^+$ and $(Ph_3PCH_2CH_2PPh_3)^{2+}$ salts.

cluster was treated with triphenylphosphine yielded no substitution products.

From the X-ray data that has been obtained, it has been determined that iron is bonded to molybdenum through sulfur linkages, but little else can be hypothesized.

Further work is necessary to obtain better crystals in order to complete the crystal structure determination.

VI. CONCLUSIONS AND PLANS FOR FUTURE WORK

A novel molybdenum-iron-sulfur cluster has been prepared and partially characterized. The available data suggest the formulation of $[MoFe_6S_6(CO)_{18}]^{2-}$ for the complex. As such, it apparently represents the first example of a new structural class of molybdenum-iron-sulfur cluster (the others are the linear and cubane clusters discussed earlier).

To eliminate any speculation, a crystal structure determination is absolutely necessary. Future work will be focussed on growing better crystals in order to reach this goal. When the structure has been determined, the next step will be to study the reactivity of the cluster.

Its use as a possible starting material to prepare new clusters more relevant to the iron-molybdenum cofactor should prove to be very interesting. Another student in the research group (G. Lilley) has recently developed a mild method for oxidative decarbonylation of M-S-CO clusters under reducing conditions. Application of this method, which involves treatment with thiolate-disulfide mixtures to this compound, should lead to a new branch of molybdenum-iron-sulfur cluster synthesis.

REFERENCES

REFERENCES

1. Schrauzer, G. N. Chemistry 50, 13 (1977).

2. Orme-Johnson, W. H.; Davis, L. C.; Henzl, M. T.; Averill, B. A.; Orme-Johnson, R. R.; Münck, E.; Zimmerman, R. Components and pathways in biological nitrogen fixation, in; Recent Developments in Nitrogen Fixation, (ed.) Newton, W. E.; Postgate, Jr.; Rodriguez-Barrucco, C.; 131, New York-London, Academic Press (1977).

3. Gillum, W. O.; Mortenson, L. E.; Chen, J.-S.; Holm, R. H. J. Amer. Chem. Soc. 99, 584 (1977).

4. Shah, V. K.; Brill, W. J. Proc. Natl. Acad. Sci., USA 74, 3249 (1977).

5. Palmer, G.; Multani, J. S.; Cretney, W. C.; Zumft, W. G.; Mortenson, L. E. Arch. Biochem. Biophys. 153, 325 (1972).

6. Smith, B. E.; Lang, G. Biochem. J. 137, 169 (1974).

7. Rawlings, J.; Shaw, V. K.; Chisnell, J. R.; Brill, W. J.; Zimmermann, R.; Münck, E.; Orme-Johnson, W. H. J. Biol. Chem. 253, 1001 (1978).

8. Münck, E.; Rhodes, H.; Orme-Johnson, W. H.; Davis, L. C.; Brill, W. J.; Shaw, V. K. Biochim. Biophys. Acta. 400, 32 (1975).

9. Antonio, M. R.; Teo, B.-K.; Orme-Johnson, W. H.; Nelson, M. J.; Groh, S. E.; Lindahl, P. A.; Kauzlarich, S. M.; Averill, B. A. J. Amer. Chem. Soc. 104, 4703 (1982).

10. Wolff, T. E.; Berg, J. M.; Warrick, C.; Hodgson, K. O.; Holm, R. H. J. Amer. Chem. Soc. 100, 4630 (1978).

11. Teo, B.-K.; Averill, B. A. Biochem. Biophys. Res. Commun. 88, 1454 (1979).

12. Wolff, T. E.; Berg, J. M.; Hodgson, K. O.; Frankel, R. B.; Holm, R. H.; J. Amer. Chem. Soc. 101, 4140 (1979).

13. Wolff, T. E.; Berg, J. M.; Power, P. P.; Hodgson, K. O.; Holm, R. H.; Frankel, R. B. J. Amer. Chem. Soc. 101, 5454 (1979).

14. Wolff, T. E.; Berg, J. M.; Holm, R. H. Inorg. Chem. 20, 174 (1981).

15. Christou, G.; Garner, C. D.; Mabbs, F. E.; King, T. J.; J. Chem. Soc., Chem. Commun. 740 (1978).

16. Holm, R. H. Chem. Soc. Rev. 10, 455 (1981).

17. Christou, G.; Garner, C. D.; Mabbs, F. E.; Drew, M. G. B. J. Chem. Soc., Chem. Commun. 91 (1979).

18. Acott, S. R.; Christou, G.; Garner, C. D.; King, T. J.; Mabbs, F. E.; Miller, R. M. Inorg. Chim. Acta, 35, L337 (1979).

19. Christou, G.; Mascharak, P. K.; Armstrong, W. H.; Papaefthymiou, G. C.; Frankel, R. B.; Holm, R. H. J. Amer. Chem. Soc. 104, 2820 (1982).

20. Garner, C. D.; Acott, S. R.; Christou, G.; Collison, D.; Mabbs, F. E.; Miller, R. M.; in "Current Perspectives in Nitrogen Fixation", Gibson, A. H.; Newton, W. E., eds., Australian Academy of Science: Canberra, 40, (1981).

21. Christou, G.; Collison, D.; Garner, C. D.; Mabbs, F.E.; Petrouleas, V. Inorg. Nucl. Chem. Lett. 17, 137 (1981).

22. Wolff, T. E.; Berg, J. M.; Power, P. P.; Hodgson, K. O.; Holm, R. H.; Frankel, R. B. J. Amer. Chem. Soc. 101, 5454 (1979).

23. Wolff, T. E.; Berg, J. M.; Power, P. P.; Hodgson, K. O.; Holm, R. H.; Inorg. Chem. 19, 430 (1980).

24. Armstrong, W. H.; Holm, R. H. J. Amer. Chem. Soc. 103, 6246 (1981).

25. Armstrong, W. H.; Mascharak, P. K.; Holm, R. H. J. Amer. Chem. Soc. 104, 4373 (1982).

26. Wolff, T. E.; Berg, J. M.; Holm, R. H. Inorg. Chem. 20, 174 (1981).

27. Armstrong, W. H.; Mascharak, P. K.; Holm, R. H. Inorg. Chem. 21 1699 (1982).

28. Cramer, S. P.; Hodgson, K. O.; Gillum, W. O.; Mortenson, L. E. J. Amer. Chem. Soc. 100, 3398 (1978).

29. Cramer, S. P.; Gillum, W. O.; Hodgson, K. O.; Mortenson, L. E.; Stiefel, E. I.; Chisnell, Jr.; Brill, W. J.; Shaw, V, K. J. Amer. Chem. Soc. 100, 3814 (1978).

30. Huynh, B. H.; Münck, E.; Orme-Johnson, W. H. Biochim. Biophys. Acta 527, 192 (1979).

31. Tieckelmann, R. H.; Silvis, H. C.; Kent, T. A.; Huynh, B. H.; Waszczak, J. V.; Teo, B-K.; Averill, B. A.; J. Amer. Chem. Soc. 102, 5550 (1980).

32. Silvis, H. C.; Averill, B. A. Inorg. Chim. Acta. 54, 657 (1981).

33. Coucouvanis, D.; Simhon, E. D.; Baenziger, N. C.; Stremple, P.; Swenson, D.; Kostikas, A.; Simopoulos, A.; Petrouleas, V.; Papaefthymiou, V. J. Amer. Chem. Soc. 102, 1730 (1980).

34. Coucouvanis, D.; Simhon, E. D.; Swenson, D.; Baenziger, N. C. J. Chem. Soc., Chem. Commun. 361 (1979).

35. Coucouvanis, D.; Simhon, E. D.; Baenziger, N. C. J. Amer. Chem. Soc., 102, 6644 (1980).

36. Coucouvanis, D.; Baenziger, N. C.; Simhon, E. D.; Stremple, P.; Swenson, D.; Simopoulos, A.; Kostikas, A.; Petrouleas, V.; Papaefthymiou, V. J. Amer. Chem. Soc. 102, 1732 (1980).

37. Tieckelmann, R. H.; Averill, B. A. Inorg. Chim. Acta. 46, L35 (1980).

38. Kepert, D. L.; Mandyczewsky, R. Inorg. Chem. Vol. 7, No. 10, 2091 (1968).

39. Emptage, M. H.; Zimmerman, R.; Que, Jr., L.; Münck, E.; Hamilton, W. D.; Orme-Johnson, W. H. Biochim. Biophys. Acta. 12, 495 (1977).

40. Hieber, W.; Gruber, J. Z. Anorg. Allg. Chem. 91, 296 (1958).

41. Seyferth, D.; Henderson, R. S.; Song, L. Organometallics 1, 125 (1982).

42. Hieber, H.; Beck, W. Z. Anorg. Allg. Chem., 305, 265 (1965).

43. Stiefel, E. I. The Coordination and Bioinorganic Chemistry of Molybdenum in Progress in Organic Chemistry, Volume 22, 57, New York (1977).

44. Allen, E. A.; Brisdon, B. J.; Fowles, G. W. A. J. Chem. Soc. 4531 (1964).

45. Lilley, G.; Averill, B. A. unpublished results.

46. Allen, E. A.; Feenan, K.; Fowles, G. W. A. J. Chem. Soc. 4531 (1964).

47. Davies, C. W. The Conductivity of Solutions, John Wiley and Sons, II. New York (1933).

48. Scovell, W. M. and Spiro, T. G. Inorg. Chem. 13, 304 (1974).

49. Lever, A. B. P. Inorganic Electronic Spectroscopy, Elsevier, 273 (1968).

50. Horner, S. M.; Tyree, S. Y., Jr. Inorg. Chem. 2, 568 (1963).

51. Carmichael, W. M.; Edwards, D. A.; Walton, R. A. J. Chem. Soc. (A) 97 (1966).

52. van den Bergen, A.; Murray, K. S.; West, B. O. Austral. J. Chem. 25, 705 (1972).

53. Gütlich, P.; Link, R.; Trautwein, A. Mössbauer Spectroscopy and Transition Metal Chemistry, Springer-Verlag Berlin Heidelberg New York 19 (1978).

54. Gibb, T. C.; Greatrex, R.; Greenwood, N. N. J. Chem. Soc. (A) 1663 (1967).

55. Herber, R. H.; Kingston, W. R.; Wertheim, G. K. Inorg. Chem. 2, 153 (1963).

56. Mayerle, J. J.; Frankel, R. B.; Holm, R. H.; Ibers, J. A.; Phillips, W. D.; Weiher, F. Proc. Natl. Acad. Sci. USA 70, 2429 (1973).

57. Dickson, D. P. E.; Cammack, R. Biochem. J. 143, 763 (1974).

58. Kostikas, A.; Petrouleas, V.; Simopoulos, A.; Coucouvanis, D.; Holah, D. G. Chem. Phys. Lett. 38, 582 (1976).

59. Horn, C. J.; Brown, T. M. Inorg. Chem. 11, 1970 (1972).

60. Mitchell, P. C. H.; Williams, R. J. P. J. Chem. Soc. 4570 (1962).

61. Midollini, S.; Bacci, M. J. Chem. Soc. (A) 2964 (1970).

62. Earnshaw, A. Introduction to Magnetochemistry Academic Press, London, New York, 101, (1968).

63. Cleland, W. E.; Holtman, D.; Sabat, M.; Ibers, J. A.; Averill, B. A. J. Amer. Chem. Soc., in press.

64. Dessy, R. E.; Stary, F. E.; King, R. B.; Waldrop, M. J. Am. Chem. Soc., 88(3), 471 (1966).

65. Rossetti, R.; Gervasio, G. and Stanghellini, P. L. Inorganica Chim. Acta. 35, 73 (1979).